The American Journal of Human Genetics, Volume *93*

Supplemental Data

ZMYND10 Is Mutated in Primary Ciliary Dyskinesia and Interacts with LRRC6

Maimoona A. Zariwala, Heon Yung Gee, Małgorzata Kurkowiak, Dalal A. Al-Mutairi, Margaret W. Leigh, Toby W. Hurd, Rim Hjeij, Sharon D. Dell, Moumita Chaki, Gerard W. Dougherty, Mohamed Adan, Philip C. Spear, Julian Esteve-Rudd, Niki T. Loges, Margaret Rosenfeld, Katrina A. Diaz, Heike Olbrich, Whitney E. Wolf, Eamonn Sheridan, Trevor F.C. Batten, Jan Halbritter, Jonathan D. Porath, Stefan Kohl, Svjetlana Lovric, Daw-Yang Hwang, Jessica E. Pittman, Kimberlie A. Burns, Thomas W. Ferkol, Scott D. Sagel, Kenneth N. Olivier, Lucy C. Morgan, Claudius Werner, Johanna Raidt, Petra Pennekamp, Zhaoxia Sun, Weibin Zhou, Rannar Airik, Sivakumar Natarajan, Susan J. Allen, Israel Amirav, Dagmar Wieczorek, Kerstin Landwehr, Kim Nielsen, Nicolaus Schwerk, Jadranka Sertic, Gabriele Köhler, Joseph Washburn, Shawn Levy, Shuling Fan, Cordula Koerner-Rettberg, Serge Amselem, David S. Williams, Brian J. Mitchell, Iain A. Drummond, Edgar A. Otto, Heymut Omran, Michael R. Knowles, Friedhelm Hildebrandt

Supplemental Acknowledgments

We are indebted to other investigators and the coordinators of the “Genetic Disorders of Mucociliary Clearance Consortium” that is part of the Rare Disease Clinical Research Network (URL: http://rarediseasesnetwork.epi.usf.edu/gdmcc/index.htm), including Drs. Stephanie Davis, Johnny Carson, Milan Hazucha, Peadar Noone, Ms. Susan Minnix and Ms. Caroline LaFave (University of North Carolina at Chapel Hill, NC), Dr. Jeffrey Atkinson and Ms. Jane Quante (Washington University, St. Louis, Mo) and Ms. Shelley Mann (The Children’s Hospital, Aurora, Co), Ms. Andrea Henkel (National Institute of Allergy and Infectious Diseases, Bethesda, MD), Dr. Carlo Milla and Ms. Jacquelyn Zirbes (Stanford University Medical Center, Palo Alto, CA), Ms. Sharon McNamara (Children’s Hospital and Regional Medical Center, Seattle, WA), Ms. Melody Miki (The Hospital for Sick Children, Toronto, Ontario, Canada). The authors also thank Ms. Lu Huang for technical assistance; and Ms. Elizabeth Godwin, for administrative support. We thank Dr. Herbert-Joachim Boenisch and Dr. Dagmar Schütte (Städtisches Klinikum-Klinik für Kinder-und Jugendmedizin Braunschweig), Dr. Johannes Wildhaber (Universitäts Kinderklinik Zürich), and Drs. Soliman Alkrinawi and Micha Aviram (Soroka University Medical Center, Beer Sheva, Israel). In addition, this publication was made possible by grants from ORDR, NHLBI and NCATS, components of National Institute of Health (NIH). Its contents are solely the responsibility of the authors and do not necessarily represent the official view of NCRR or NIH. Z.S. is supported by core A (1P30DK090744-01) and ACS (RSG-10-247-01-DDC). F.H. is an Investigator of the Howard Hughes Medical Institute and a Doris Duke Distinguished Clinical Scientist. K.N.O. is supported by the Intramural Research Program of the National Institute of Allergy and Infectious Diseases, NIH.

(A) A4197 (#8) *DNAH5* **[c.1090-6A>G, splice (het); p.Phe2077Ser (het)]**

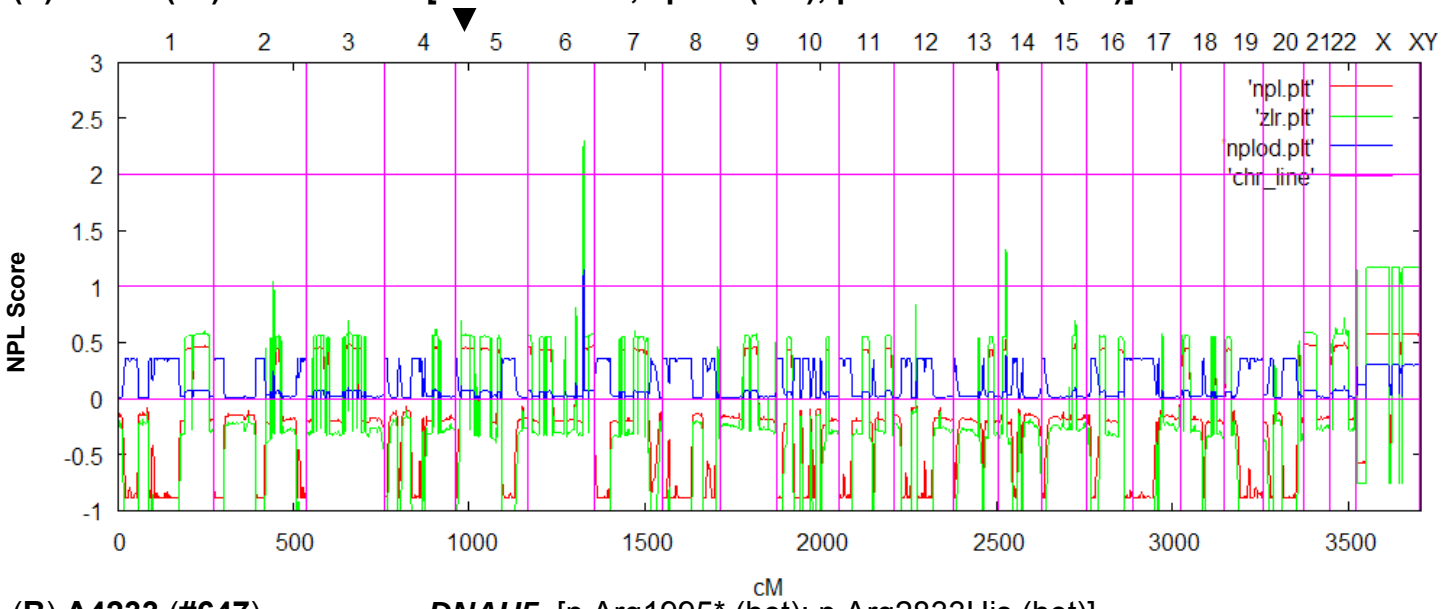

(B) **A4233 (#647)** ***DNAH5*** [p.Arg1995* (het); p.Arg2833His (het)]

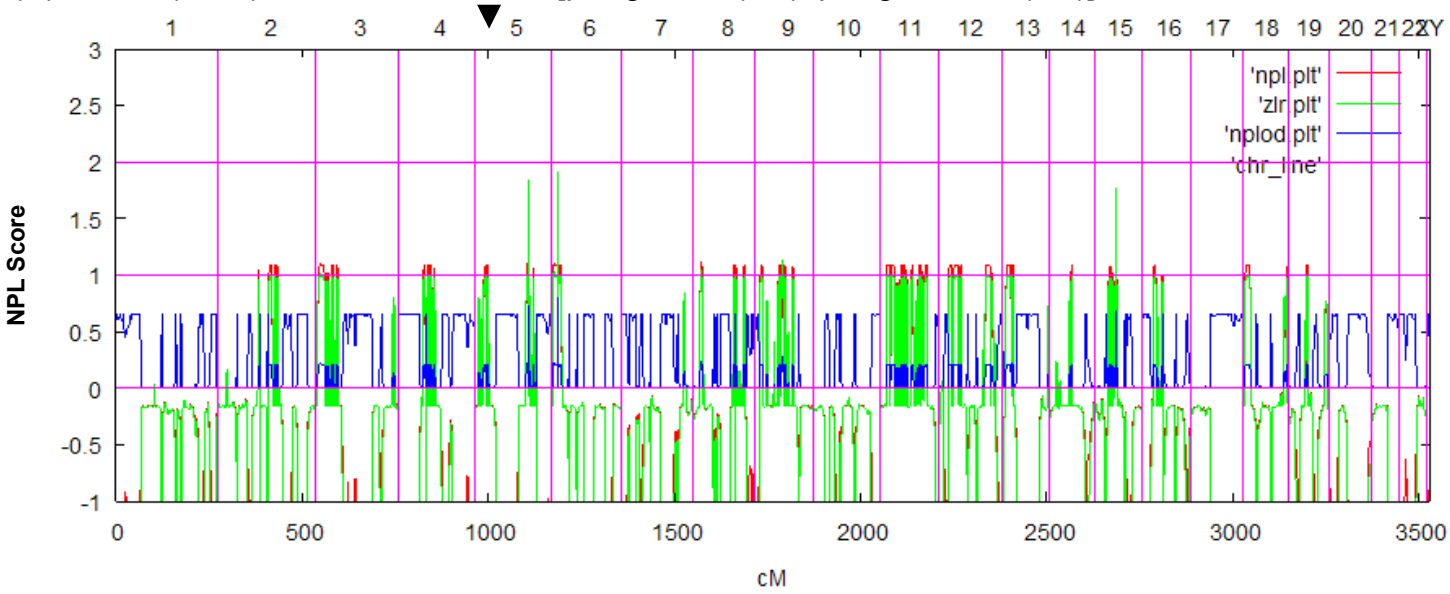

(C) **A4201 (#20)** ***DNAH5*** [p.Gln3462* (het); p.Met2083Ile, splice (het)]

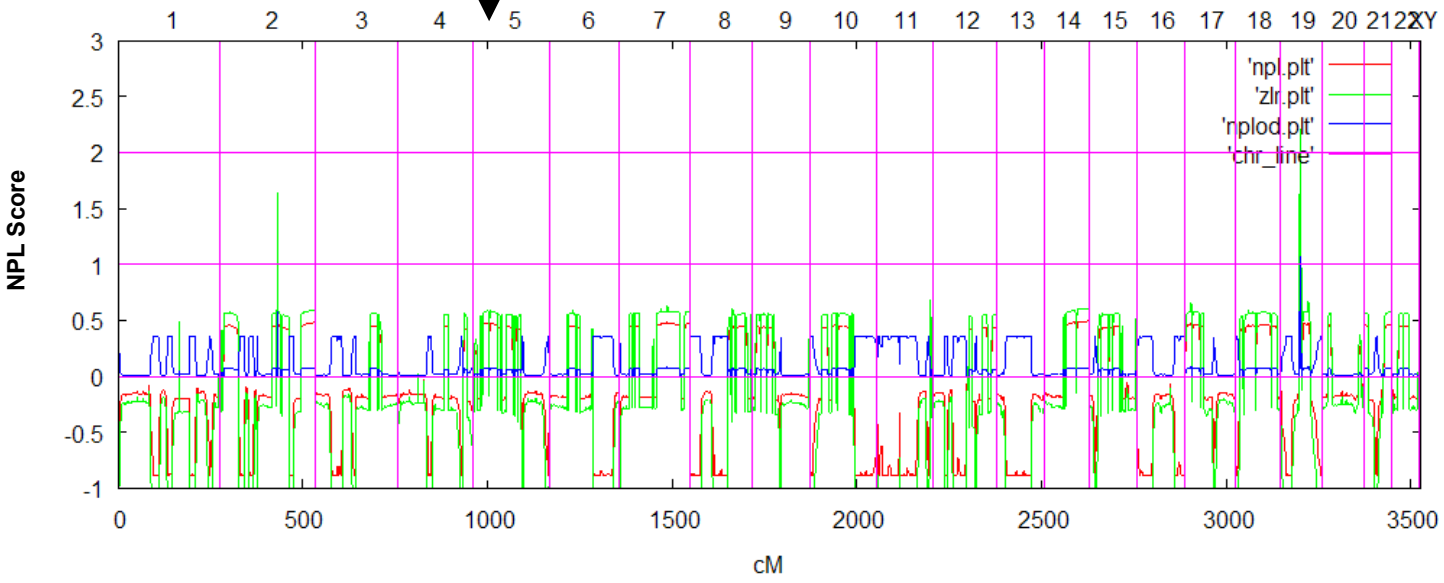

(D) **A4207** (**#100**) ***DNAH5*** [p.Lys3143* (het); p.Arg3539Cys (het)]

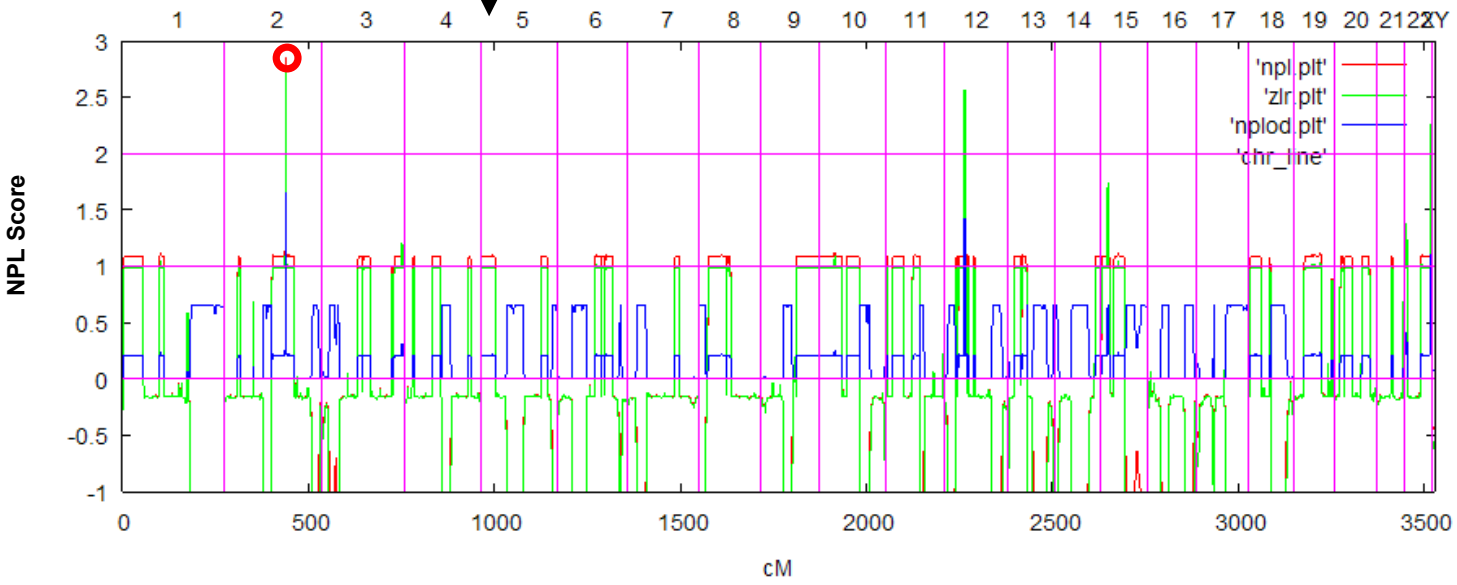

(E) **A4200** (**#11**) ***DNAH5*** [p.Gln3462* (Hom)]

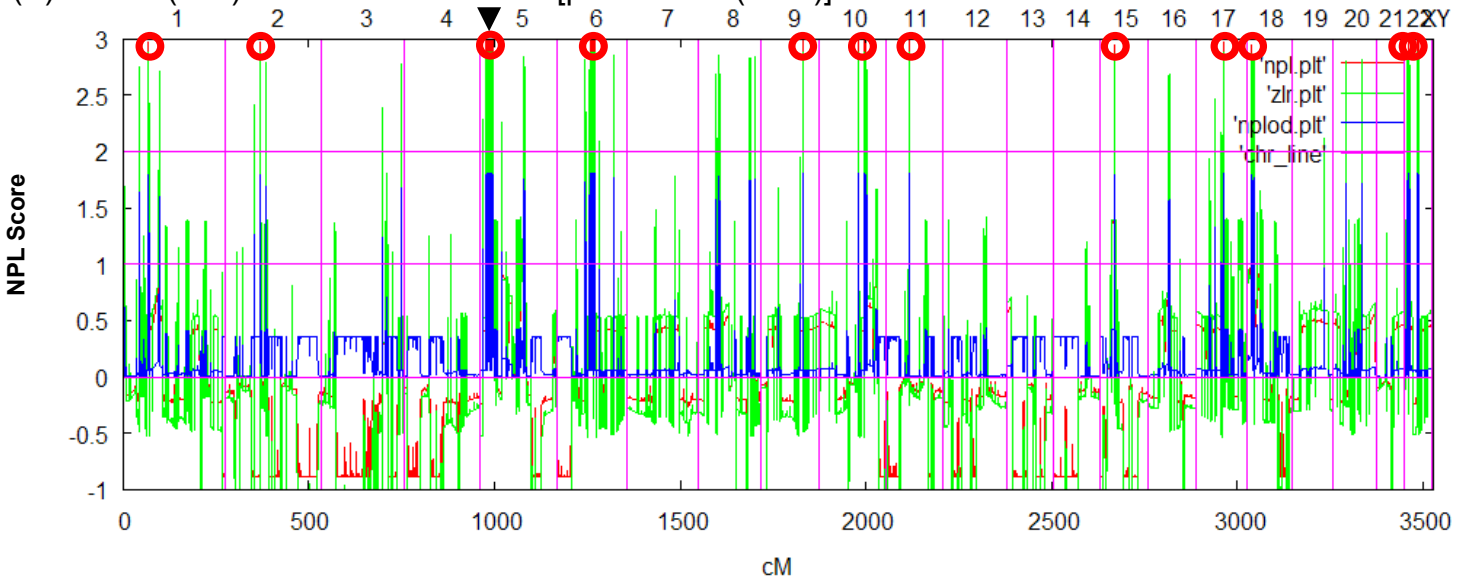

(F) **A4293** (**#1**) ***CCDC39*** [c.610-2A>G, splice (het); p.Thr277Argfs*3 (het)]

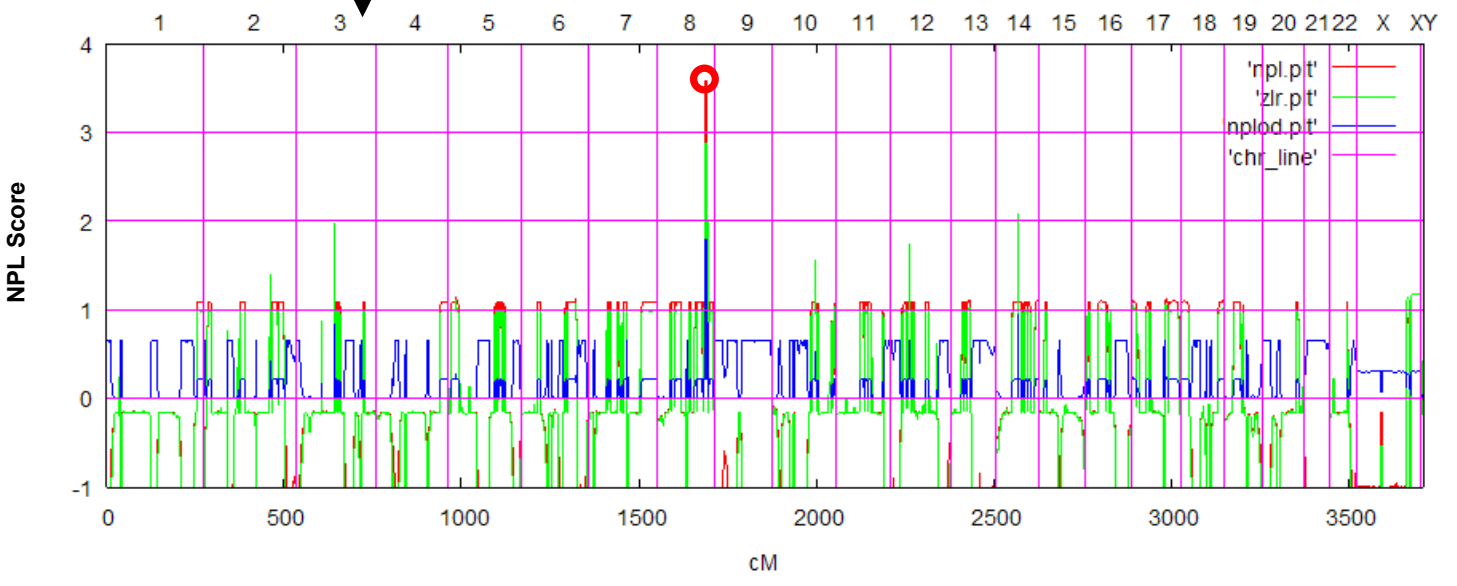

(**G**) **A4195** (**#2**) ***CCDC39*** [p.Phe514Glnfs*5 (het); c.1528-43A>G, splice (het)]

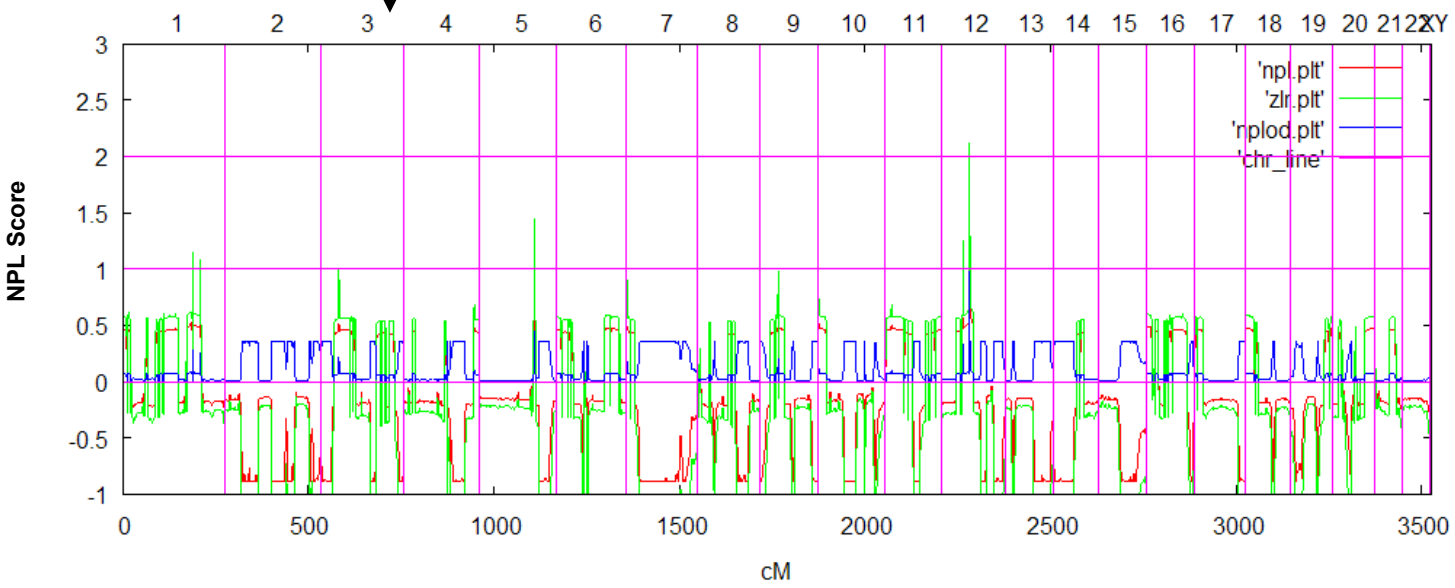

(**H**) **A4199** (**#10**) ***CCDC39*** [p.Glu597* (het); p.Gln833Valfs*6 (het)]

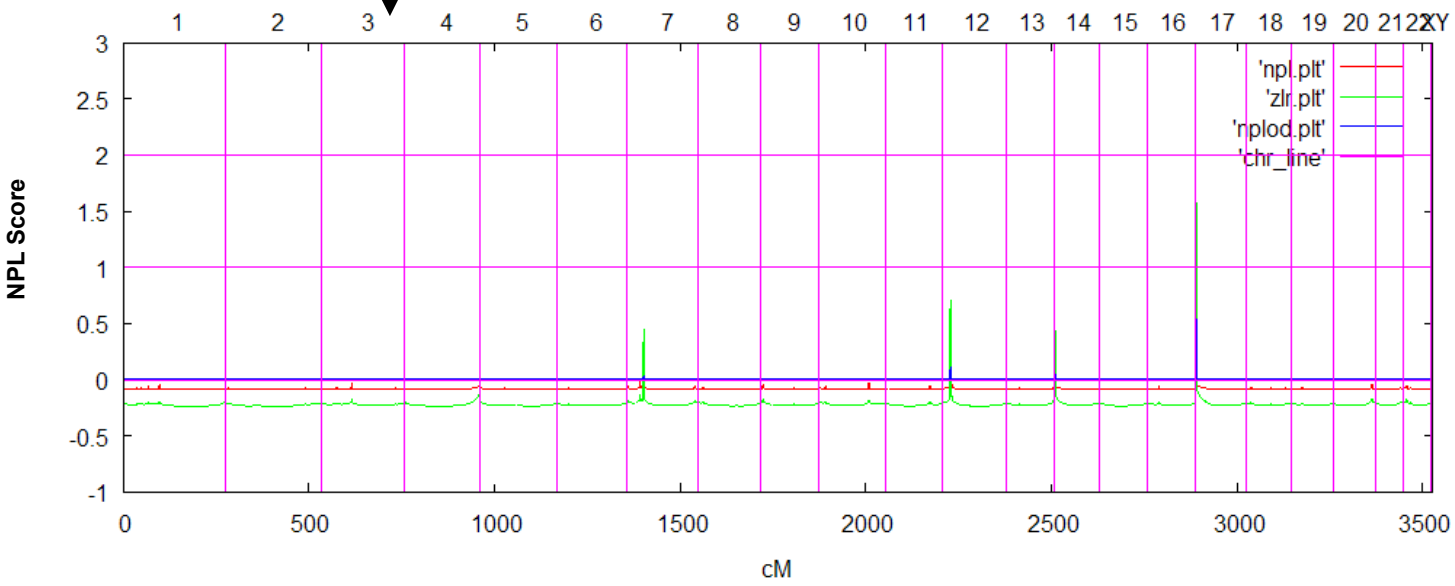

(**I**) **A4220** (**#337**) ***CCDC40*** [p.Ala83Valfs*84 (hom)]

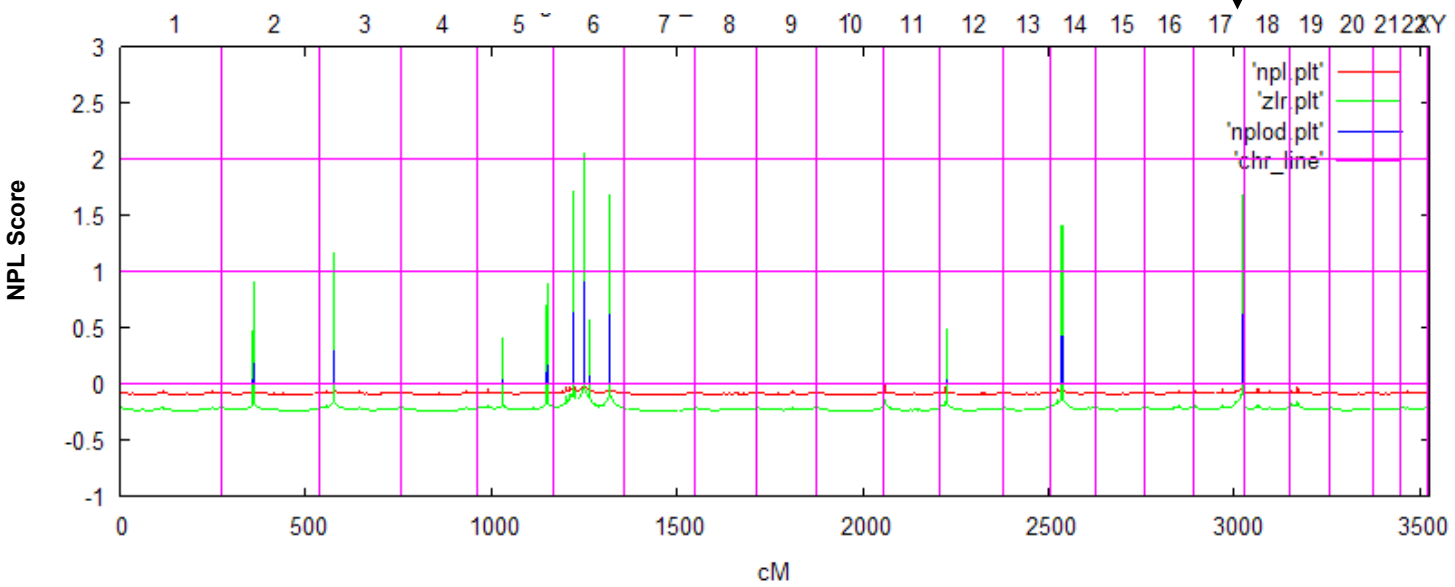

(J) **A4216 (#250)**

CCDC40 [p.Ile473Phefs*2 (hom)]

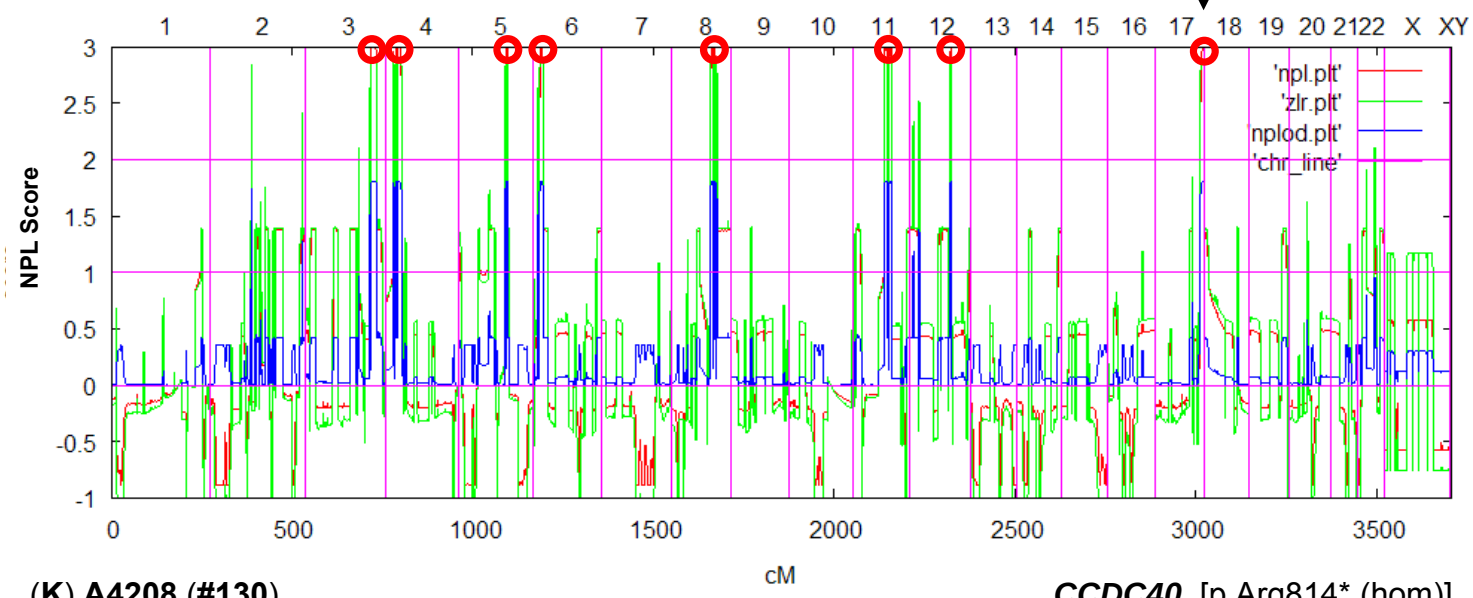

(K) **A4208 (#130)**

CCDC40 [p.Arg814* (hom)]

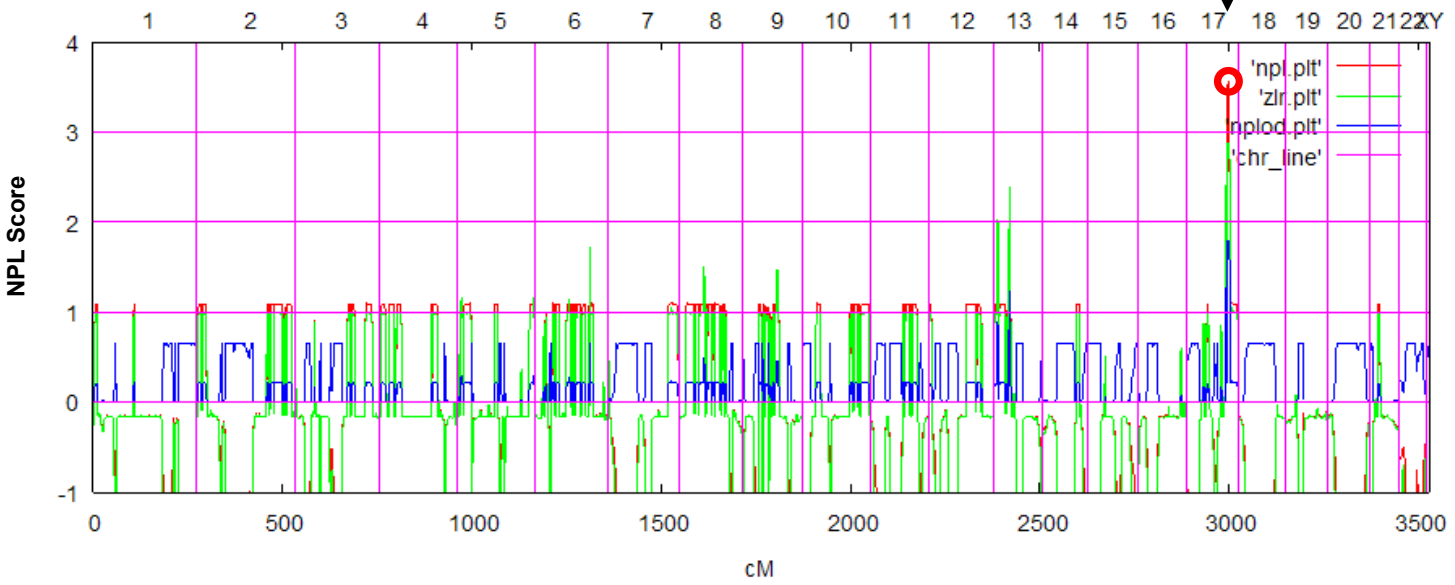

(L) **A4224 (#394/527)**

DNAH11 [p.Gln831* (het);p.Ala1291Thr (het)]

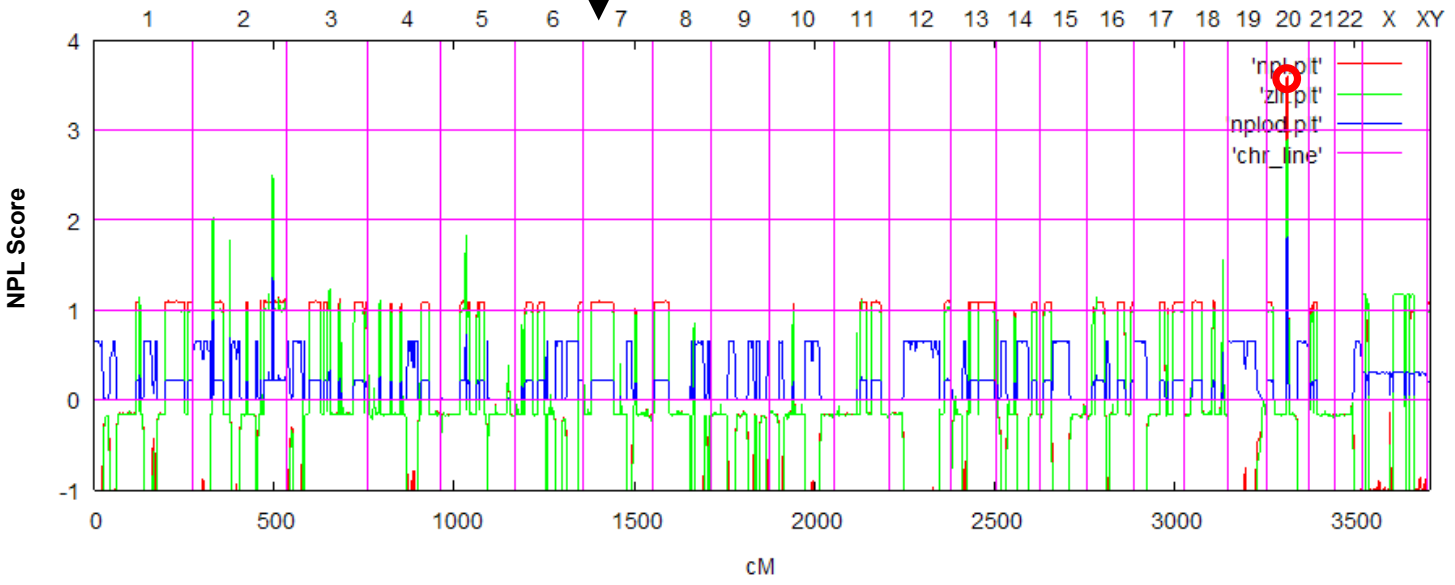

(**M**) **A4230** (**#560**) ***DNAH11*** [p.Arg1485* (het);p.Arg2907* (het)]

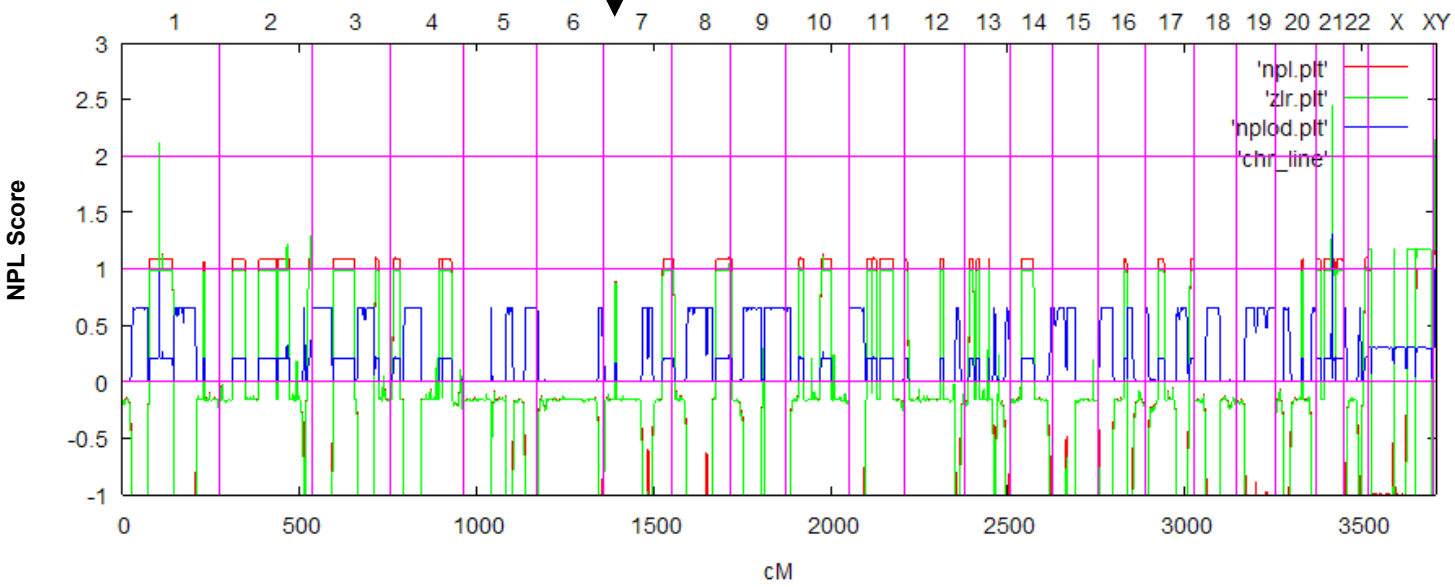

(**N**) **A4218** (**#268**) ***DNAI2*** [p.Trp435* (het); p.Glu453Glyfs*40 (het)]

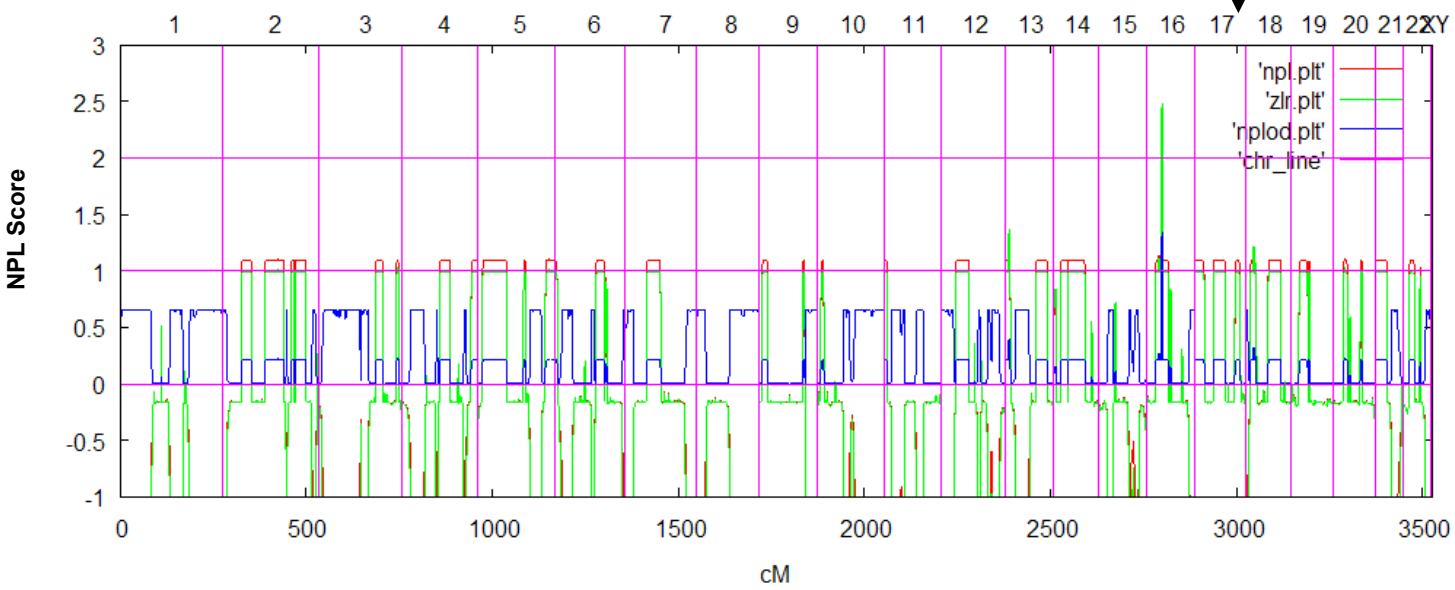

(**O**) **A4217** (**#264**) ***CCDC103*** [p.His154Pro (hom)]

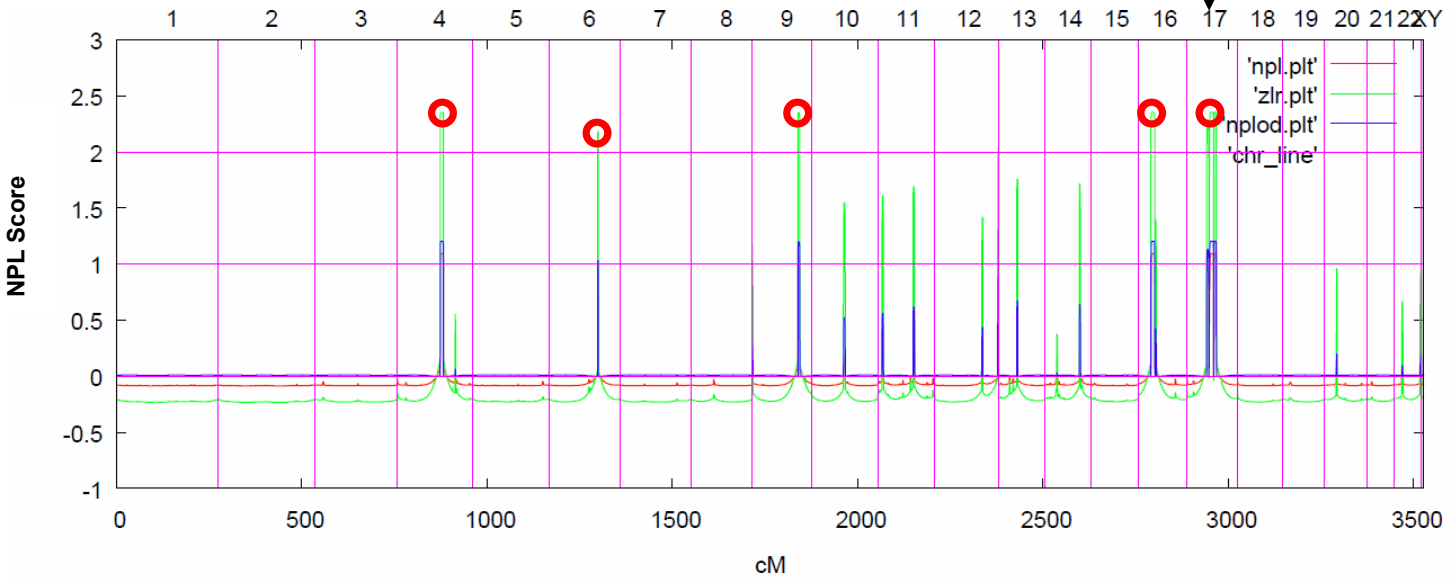

(P) **A4228 (#530/1674)** ***DNAH5*** [p.Gln1413* (het)]

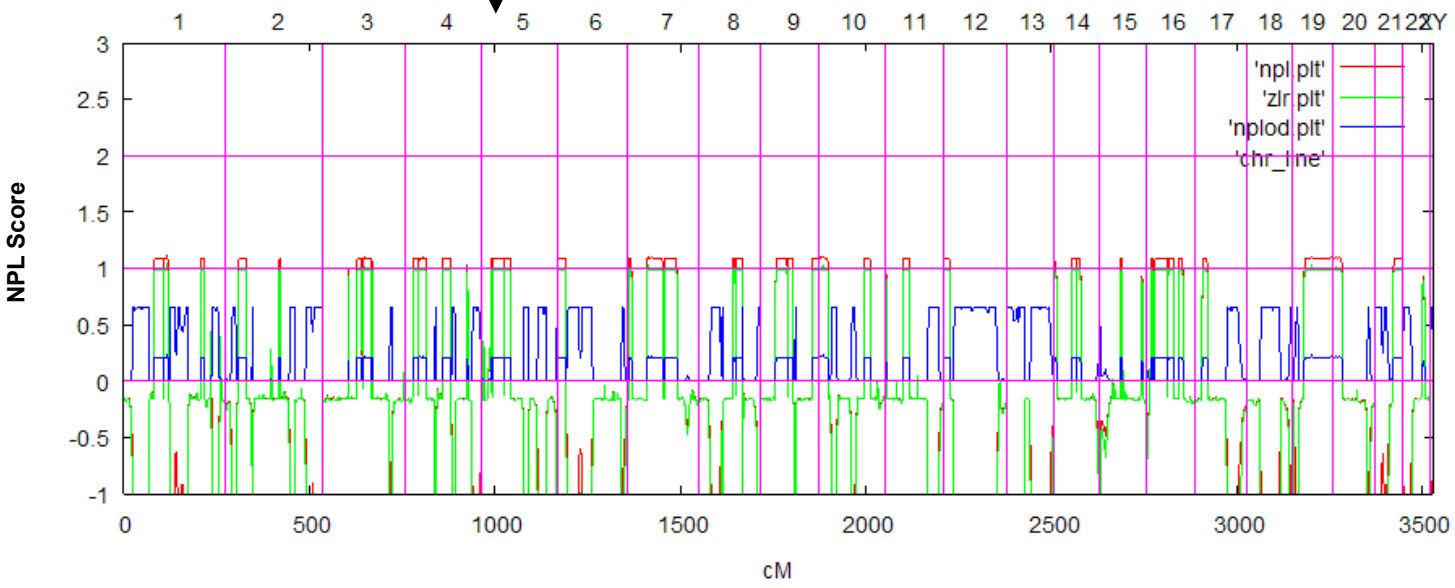

(Q) **A4198 (#9)** ***DNAH5*** [p.Arg1883* (het)]

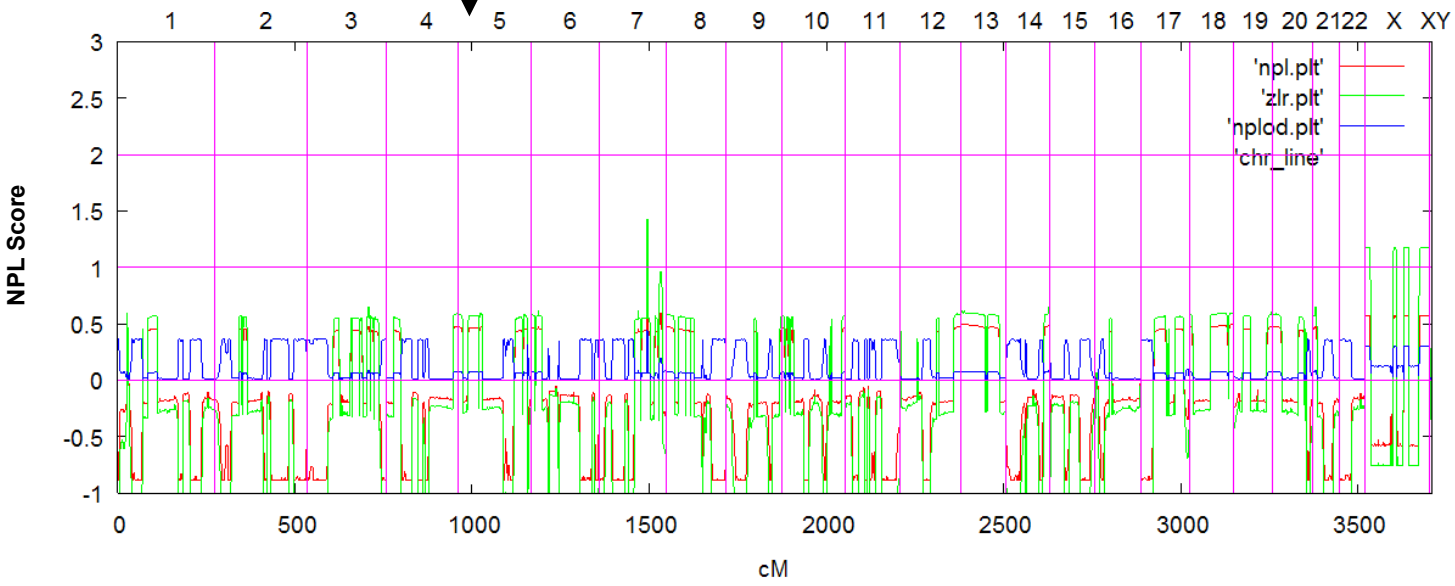

(R) **A4221 (#348)** ***DNAH5*** [c.8449-2A>G, splice (het)]

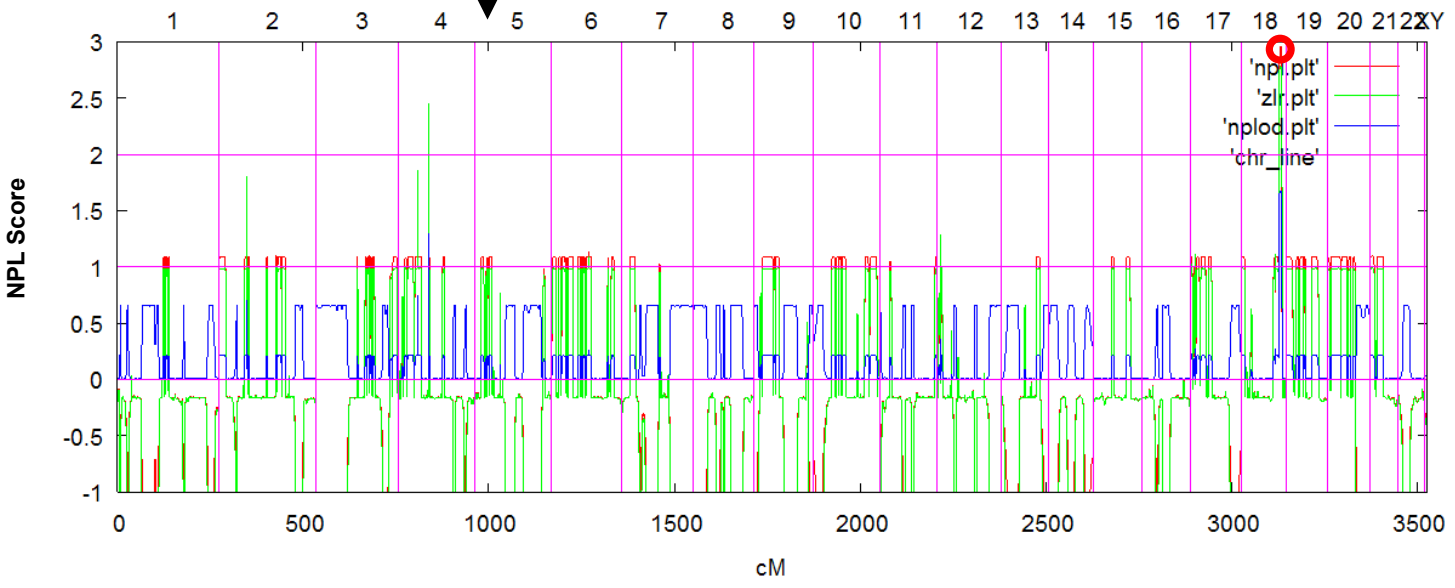

(S) **A4213 (#232)** ***LRRC6*** [p.Trp210Cysfs*12 (hom)]

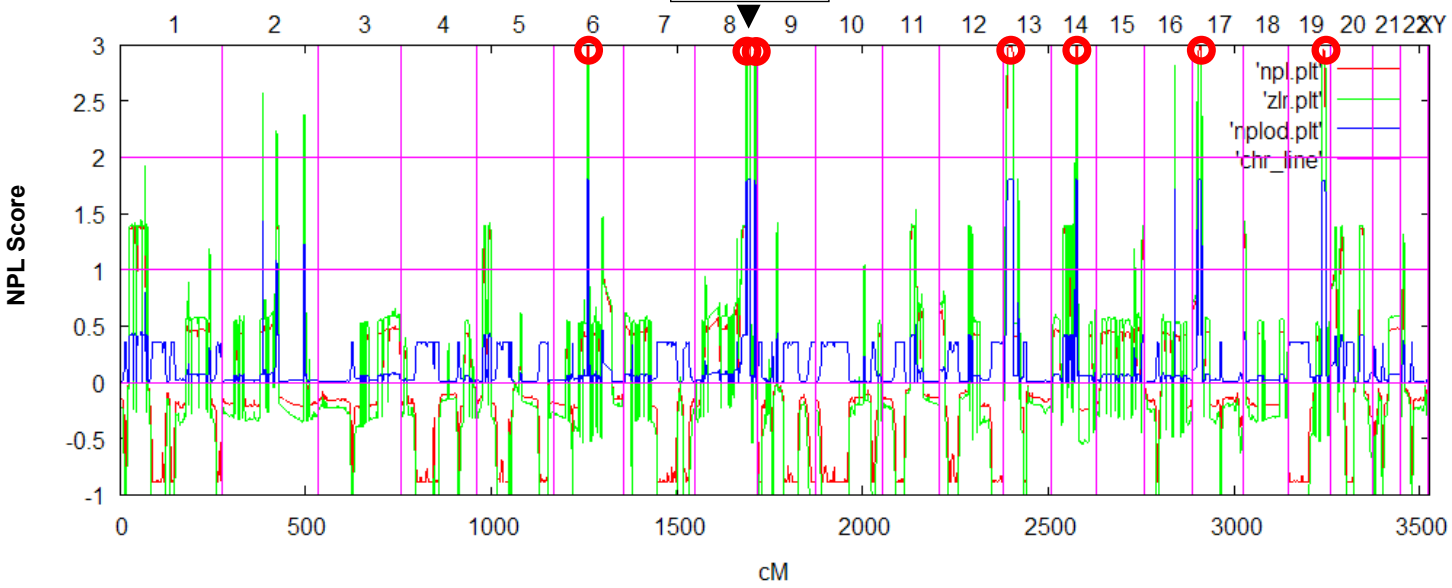

(T) **A4231 (#568)** ***ZMYND10*** [p.Tyr379Cys (hom)]

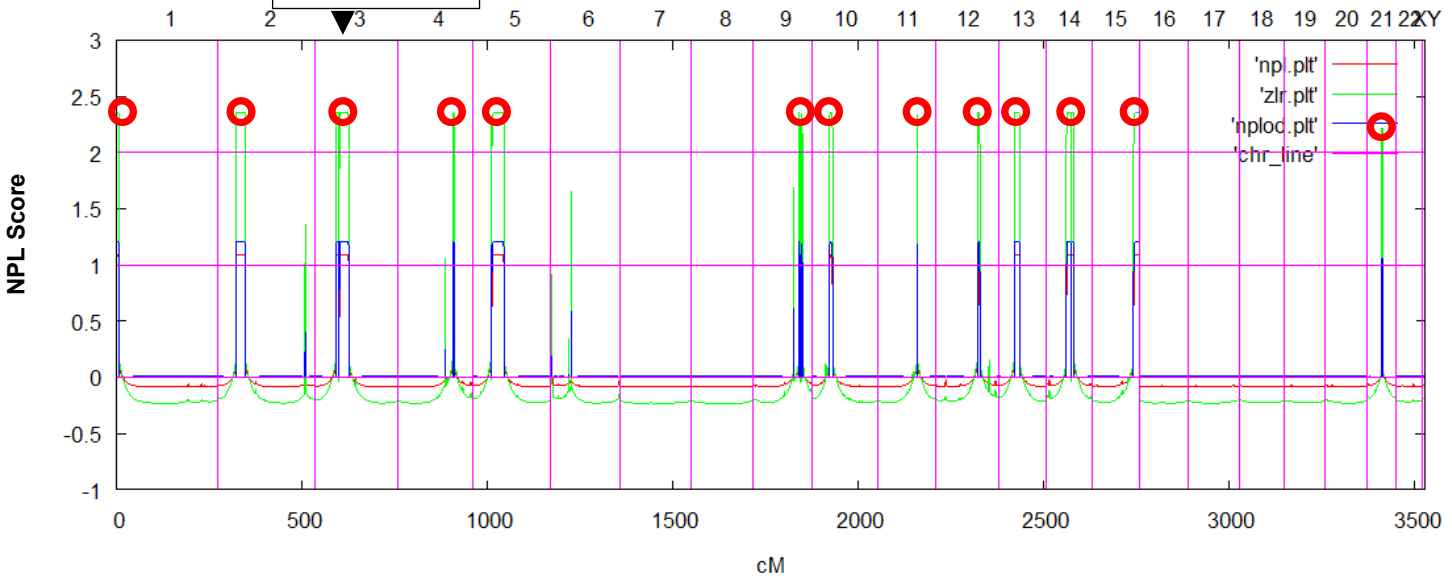

(U) **A4225 (#400)**

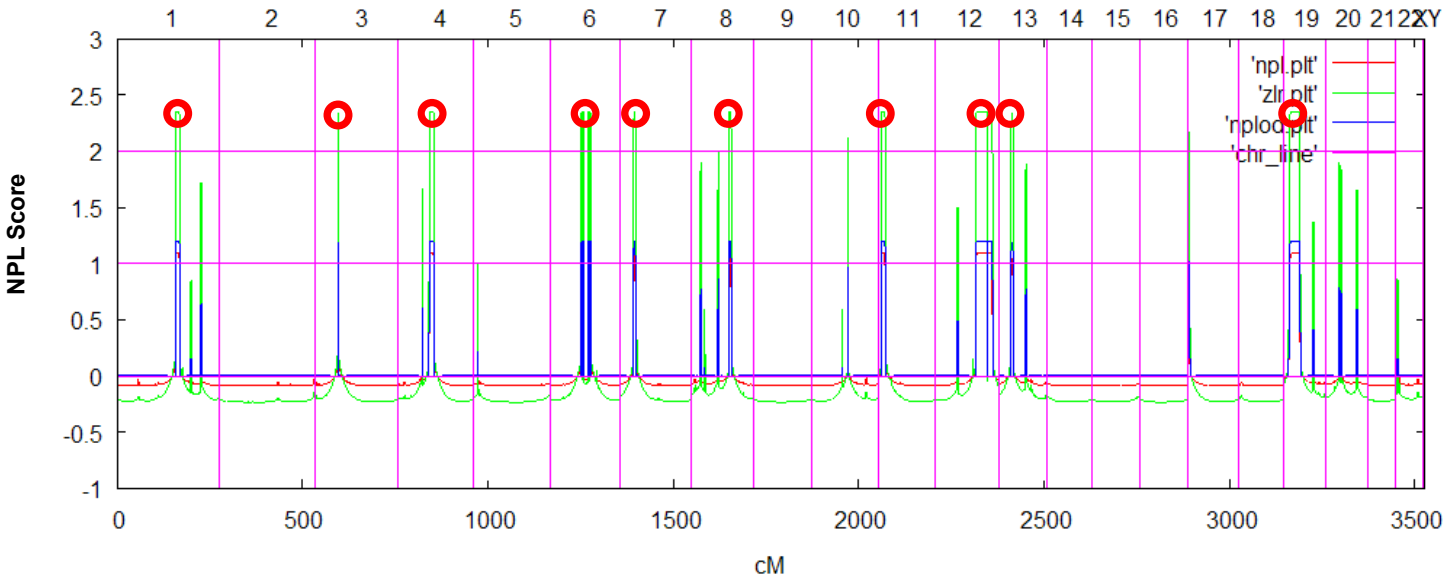

(V) A4214 (#233)

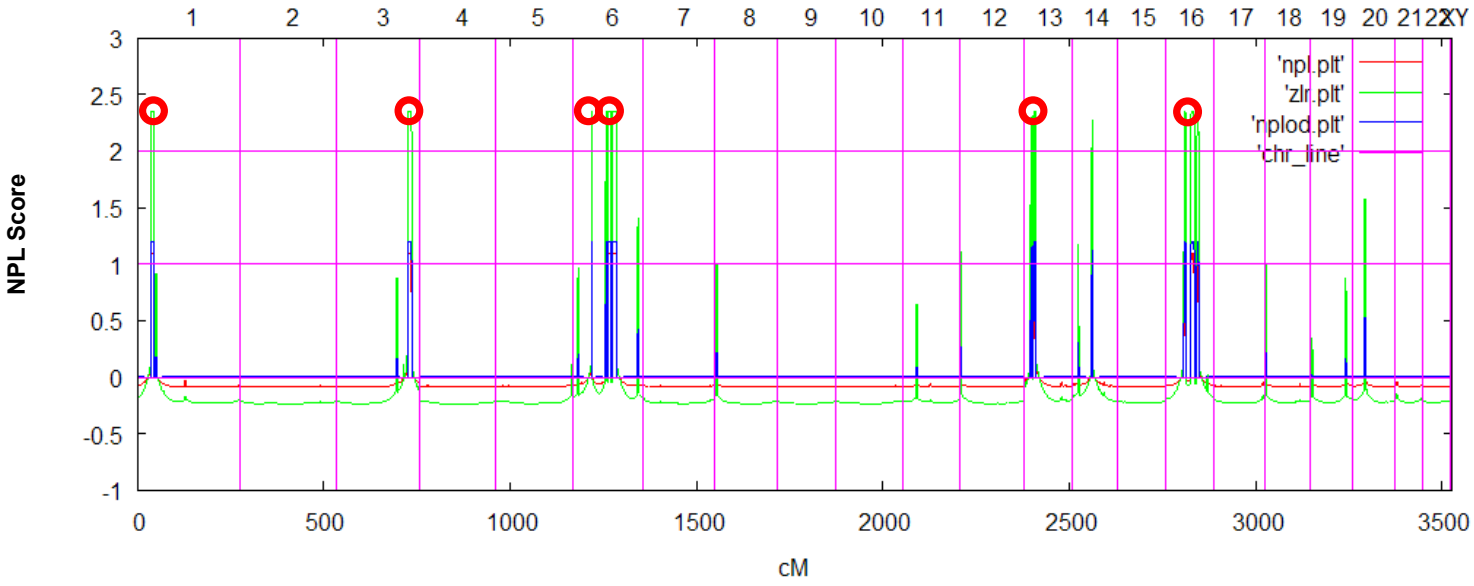

(W) A4211 (#160)

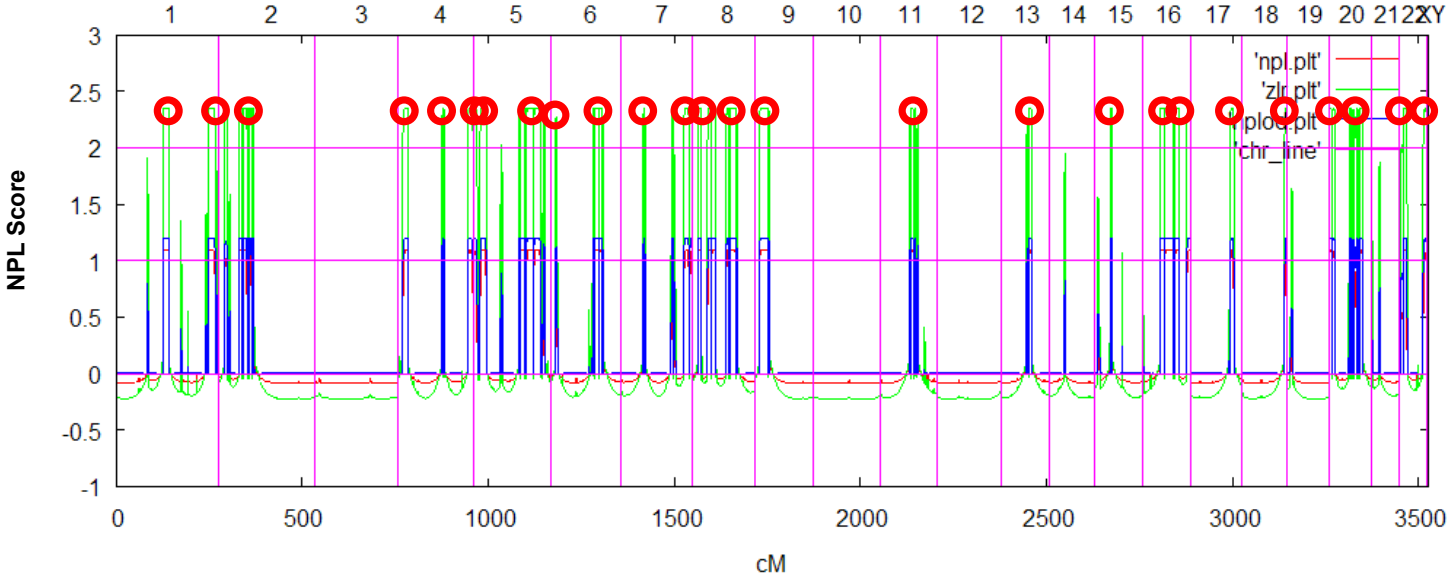

(X) A4209 (#131)

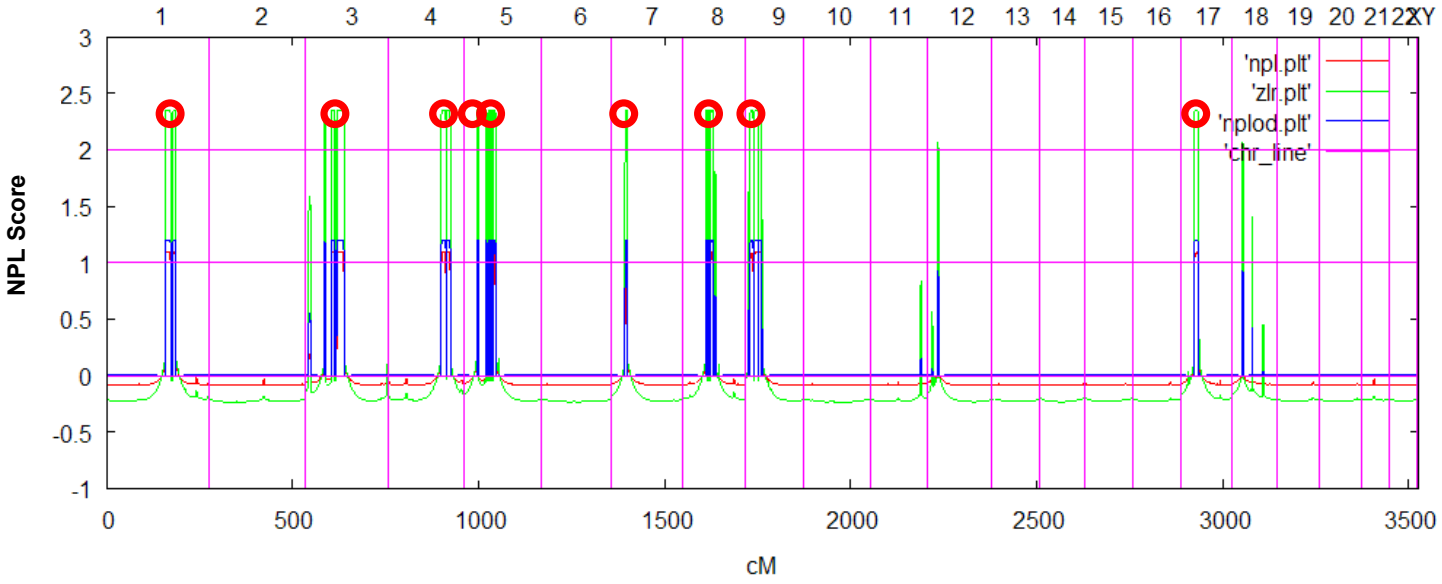

(Y) **A4206 (#66)**

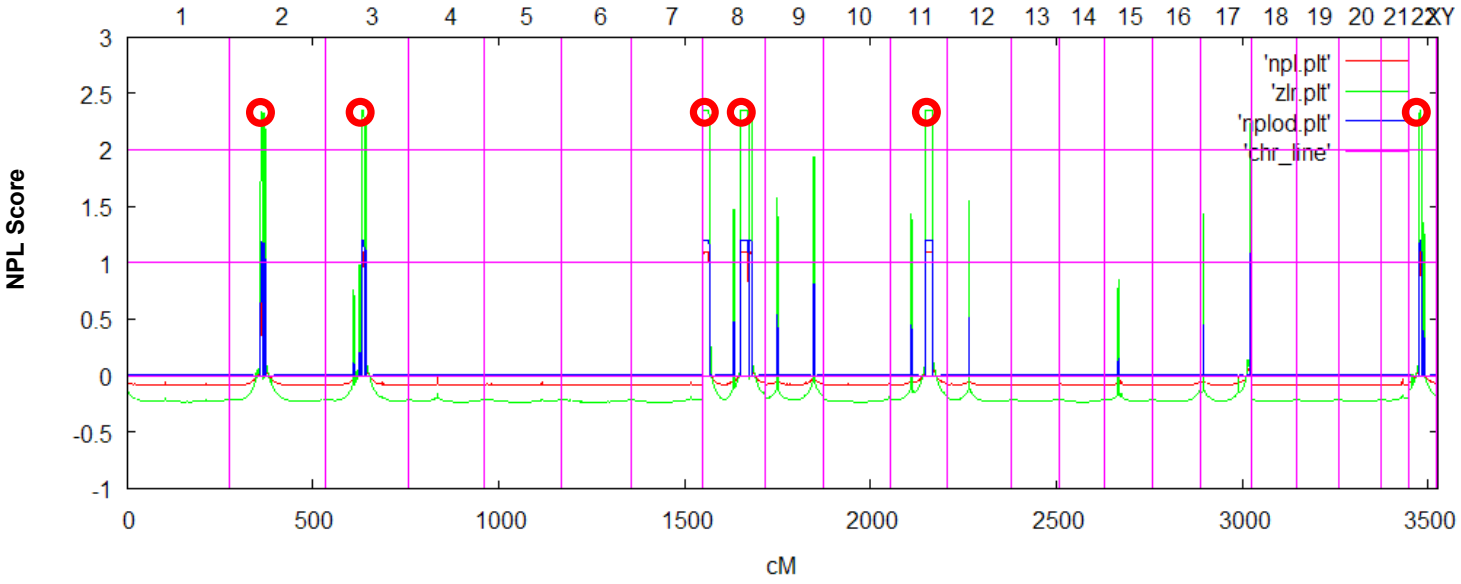

(Z) **A4219 (#287)**

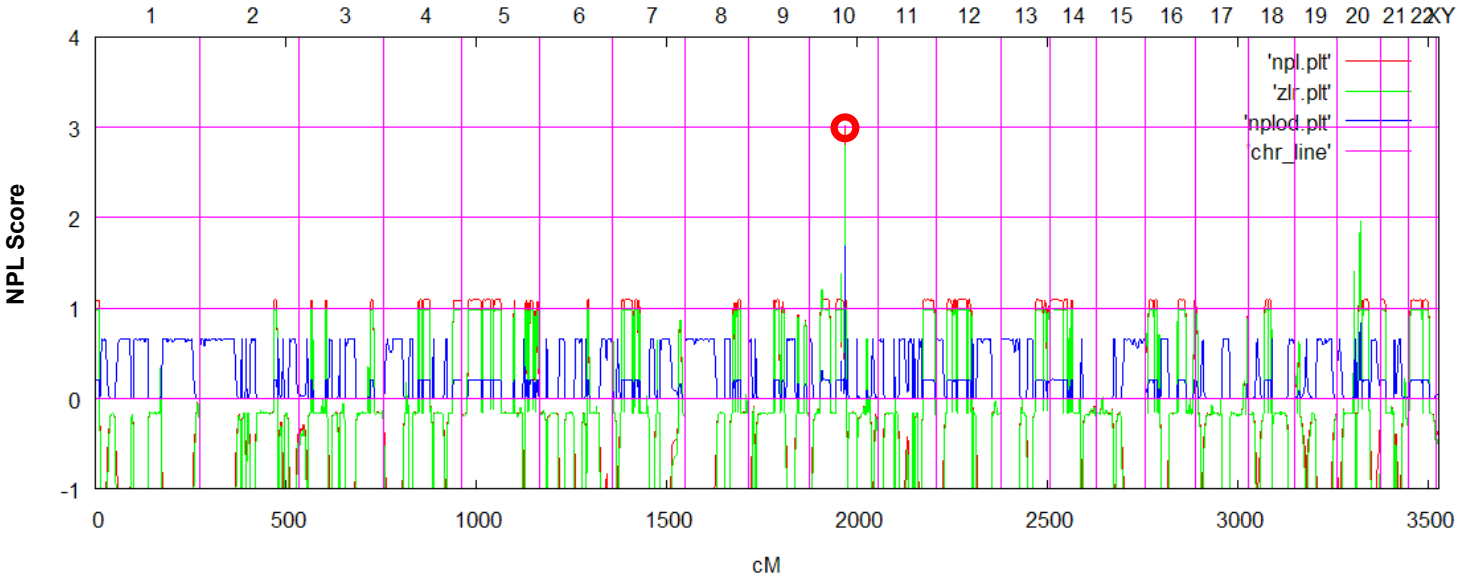

(Z1) **A4294 (#22)**

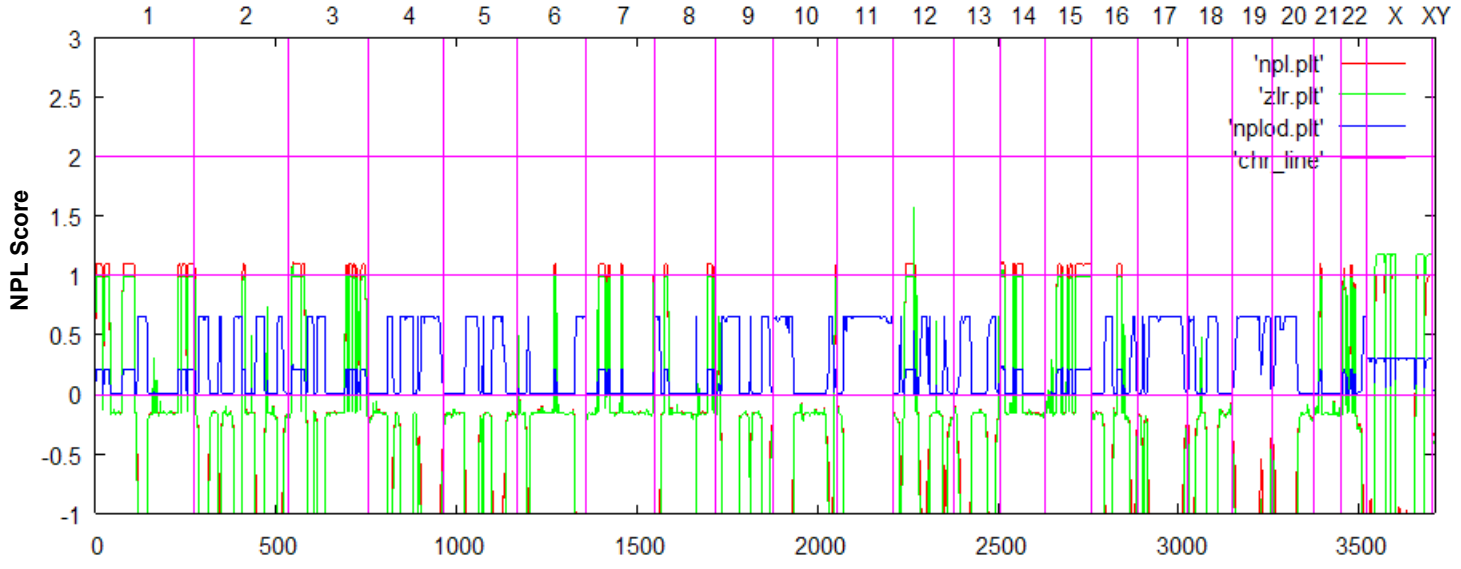

(Z2) A4203 (#28)

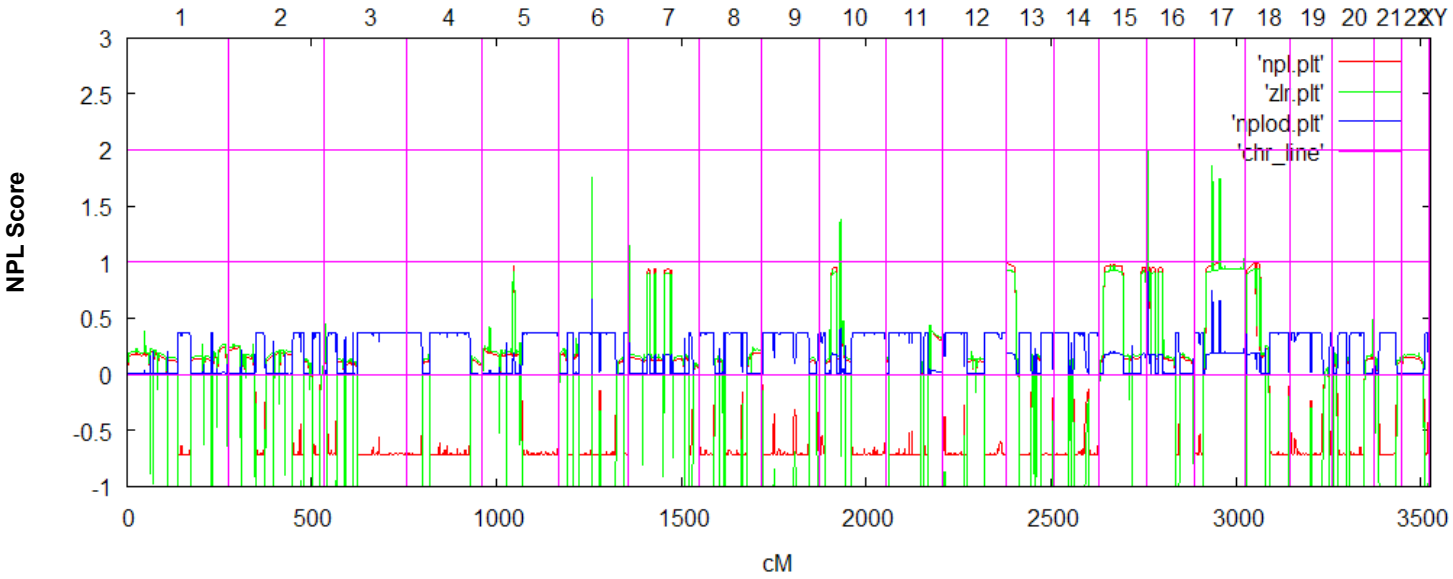

(Z3) A4226 (#495)

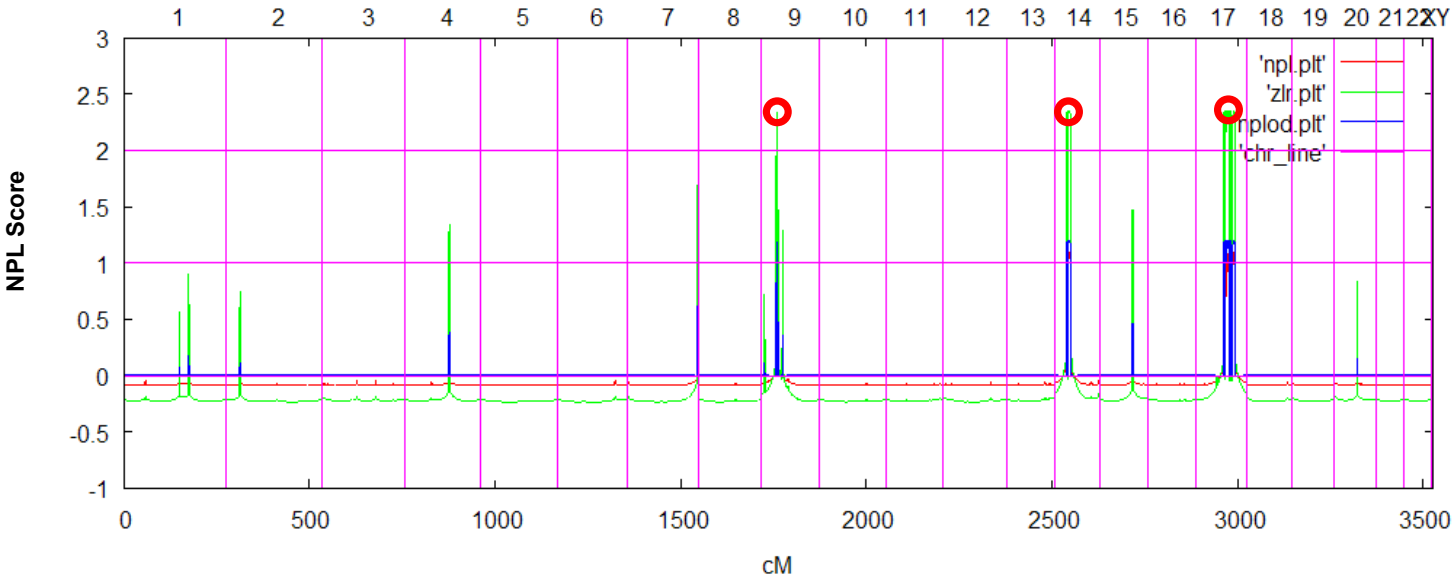

(Z4) A4227 (#510)

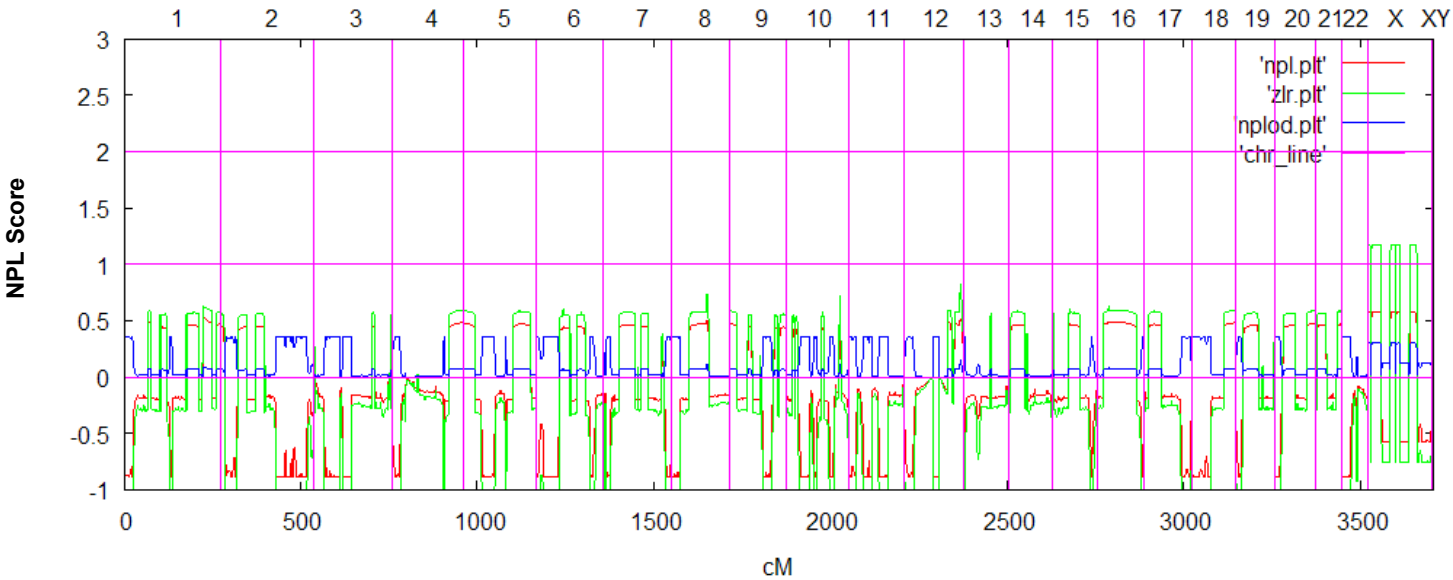

(**Z5**) **A4298** (**#651**)

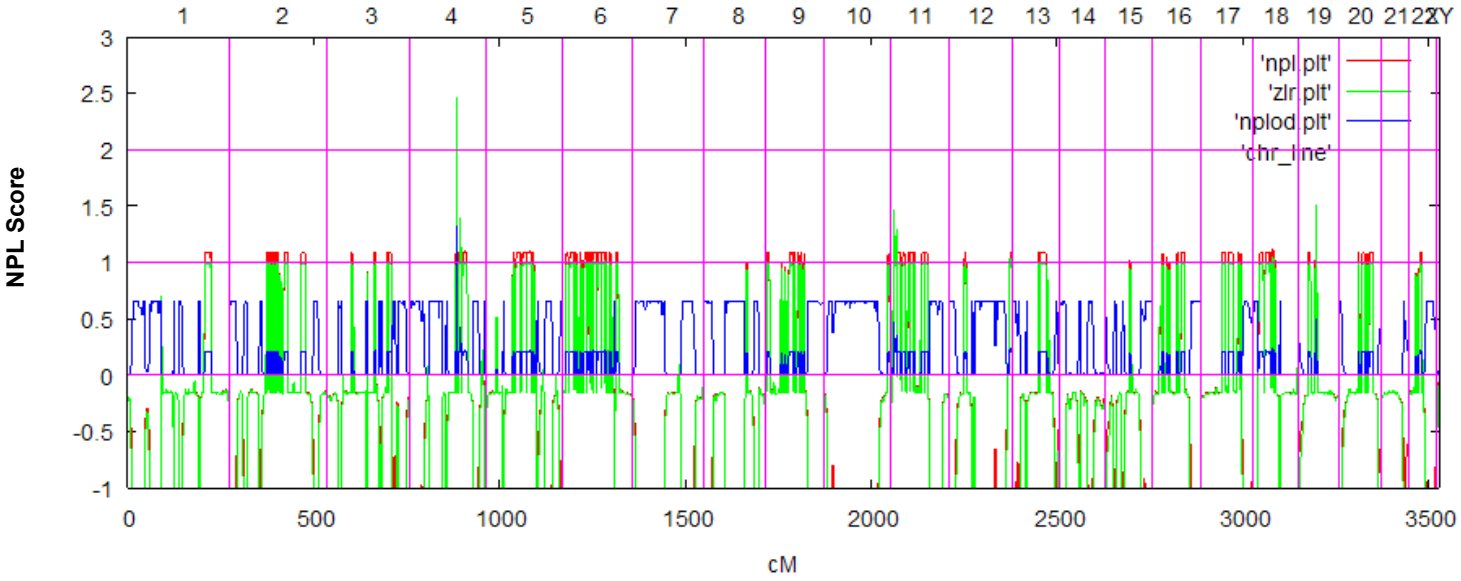

Figure S1. Homozygosity Mapping and Position of Causative Gene Mutations in 31 Patients/Families with Primary Cilia Dyskinesia (PCD)

Homozygosity profiles are shown for 21 sib pairs and 10 single individuals with PCD. Non-parametric LOD scores (NPL Score) were calculated for both affected siblings together (or for single affecteds) as described in Hildebrandt *et al.*, *PLoSGenet* 5:e1000353, 2009. using ALLEGRO[12] and assuming first-degree cousin consanguinity of the parents. Non-parametric LOD scores were plotted over genetic distance across the genome, where chromosomal positions are concatenated from p to q-arm (left to right). “Homozygosity peaks” (red circles) represent possible segments of homozygosity by descent, one of which (arrow head) harbors the disease-causing gene in each patient (see **Table 1**, **Table S1** and **Table S2**). Plots are listed in the same order of families as in **Table S1.** Headings depict family identifier, *gene symbol*, and effect of mutation on translation product. (hom),homozygous; (het), heterozygous

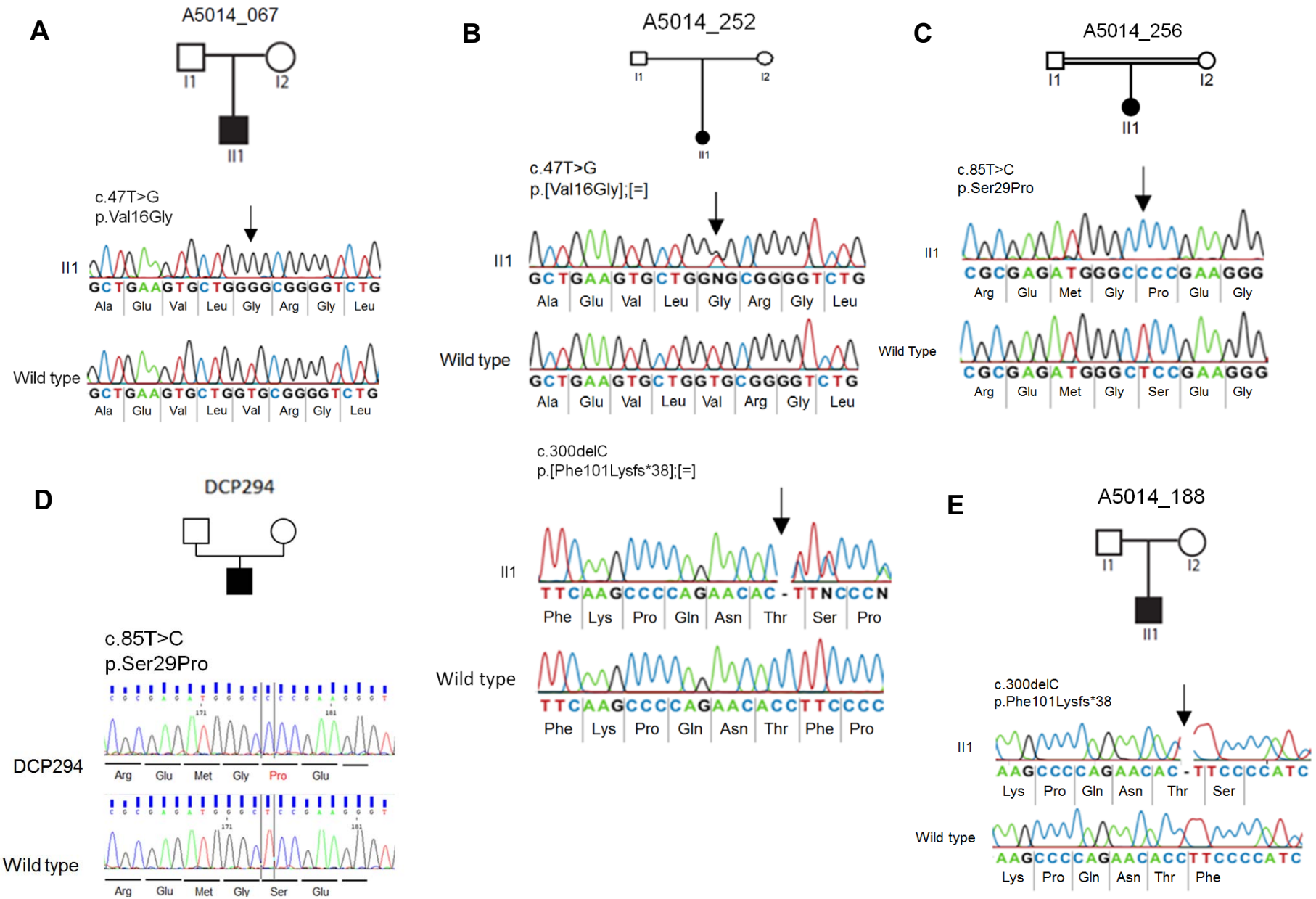
A
A5014_067
I1
I2
II1
c.47T>G
p.Val16Gly
II1
GCTGAAGTGCTGGGGCGGGGTCTG
Ala Glu Val Leu Gly Arg Gly Leu
Wild type
GCTGAAGTGCTGGTGCGGGGTCTG
Ala Glu Val Leu Val Arg Gly Leu
B
A5014_252
I1
I2
II1
c.47T>G
p.[Val16Gly];[=]
II1
GCTGAAGTGCTGGNGCGGGGTCTG
Ala Glu Val Leu Gly Arg Gly Leu
Wild type
GCTGAAGTGCTGGTGCGGGGTCTG
Ala Glu Val Leu Val Arg Gly Leu
c.300delC
p.[Phe101Lysfs*38];[=]
II1
TTCAAGCCCCAGAACAC-TTNCCCN
Phe Lys Pro Gln Asn Thr Ser Pro
Wild type
TTCAAGCCCCAGAACACCTTCCCC
Phe Lys Pro Gln Asn Thr Phe Pro
C
A5014_256
I1
I2
II1
c.85T>C
p.Ser29Pro
II1
CGCGAGATGGGCCCCGAAGGG
Arg Glu Met Gly Pro Glu Gly
Wild Type
CGCGAGATGGGCTCCGAAGGG
Arg Glu Met Gly Ser Glu Gly
D
DCP294
c.85T>C
p.Ser29Pro
DCP294
Arg Glu Met Gly Pro Glu
Wild type
Arg Glu Met Gly Ser Glu
E
A5014_188
I1
I2
II1
c.300delC
p.Phe101Lysfs*38
II1
AAGCCCCAGAACAC-TTCCCCATC
Lys Pro Gln Asn Thr Ser
Wild type
AAGCCCCAGAACACCTTCCCCATC
Lys Pro Gln Asn Thr Phe

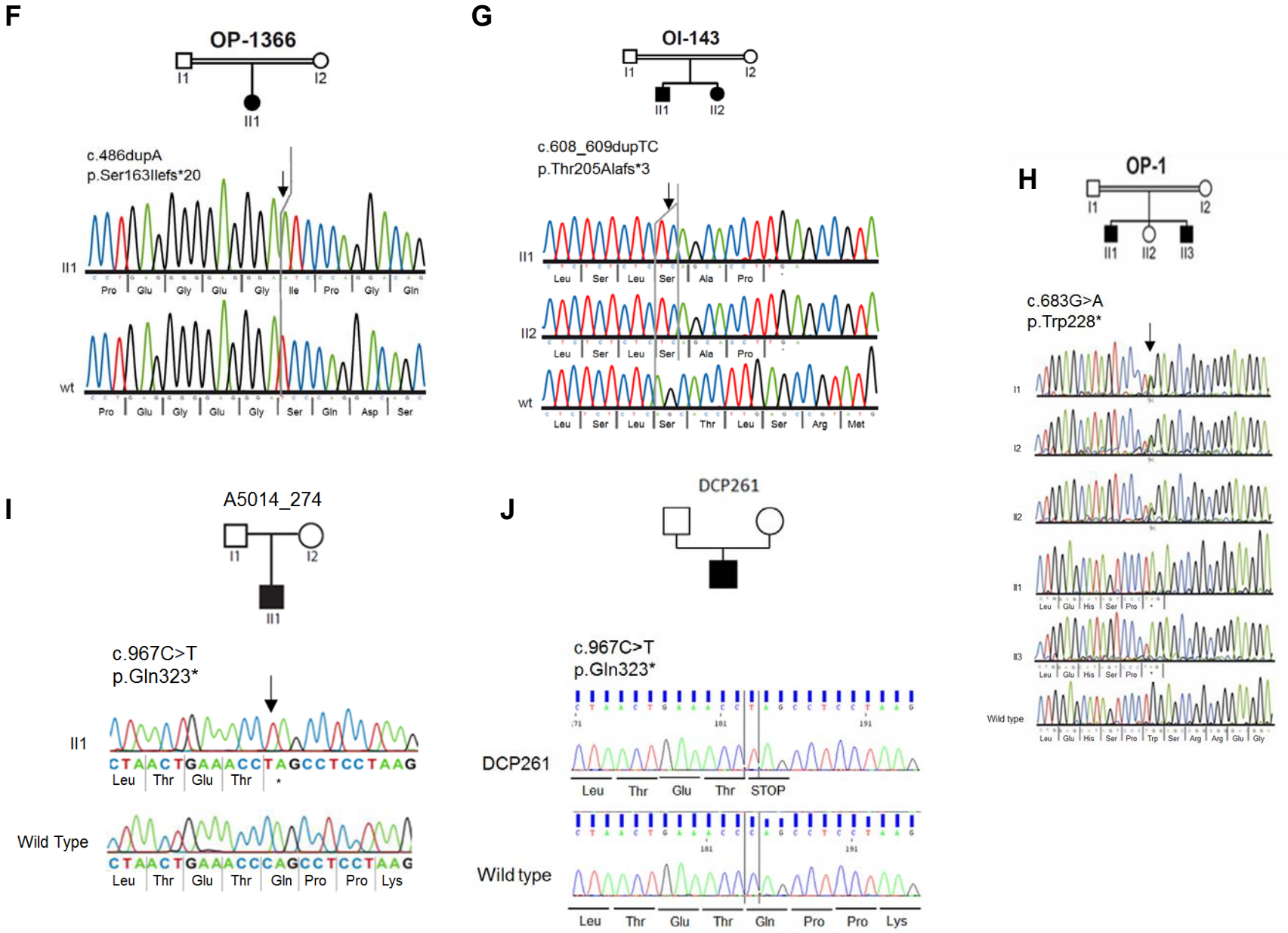
F
OP-1366
I1
I2
II1
c.486dupA
p.Ser163Ilefs*20
II1
Pro Glu Gly Glu Gly Ile Pro Gly Gln
wt
Pro Glu Gly Glu Gly Ser Gln Asp Ser
G
OI-143
I1
I2
II1
II2
c.608_609dupTC
p.Thr205Alafs*3
II1
Leu Ser Leu Ser Ala Pro
II2
Leu Ser Leu Ser Ala Pro
wt
Leu Ser Leu Ser Thr Leu Ser Arg Met
H
OP-1
I1
I2
II1
II2
II3
c.683G>A
p.Trp228*
I1
I2
II2
II1
Leu Glu His Ser Pro
II3
Leu Glu His Ser Pro
Wild type
Leu Glu His Ser Pro Trp Ser Arg Arg Glu Gly
I
A5014_274
I1
I2
II1
c.967C>T
p.Gln323*
II1
CTAACTGAAACCTAGCCTCCTAAG
Leu Thr Glu Thr *
Wild Type
CTAACTGAAACCCAGCCTCCTAAG
Leu Thr Glu Thr Gln Pro Pro Lys
J
DCP261
c.967C>T
p.Gln323*
DCP261
Leu Thr Glu Thr STOP
Wild type
Leu Thr Glu Thr Gln Pro Pro Lys

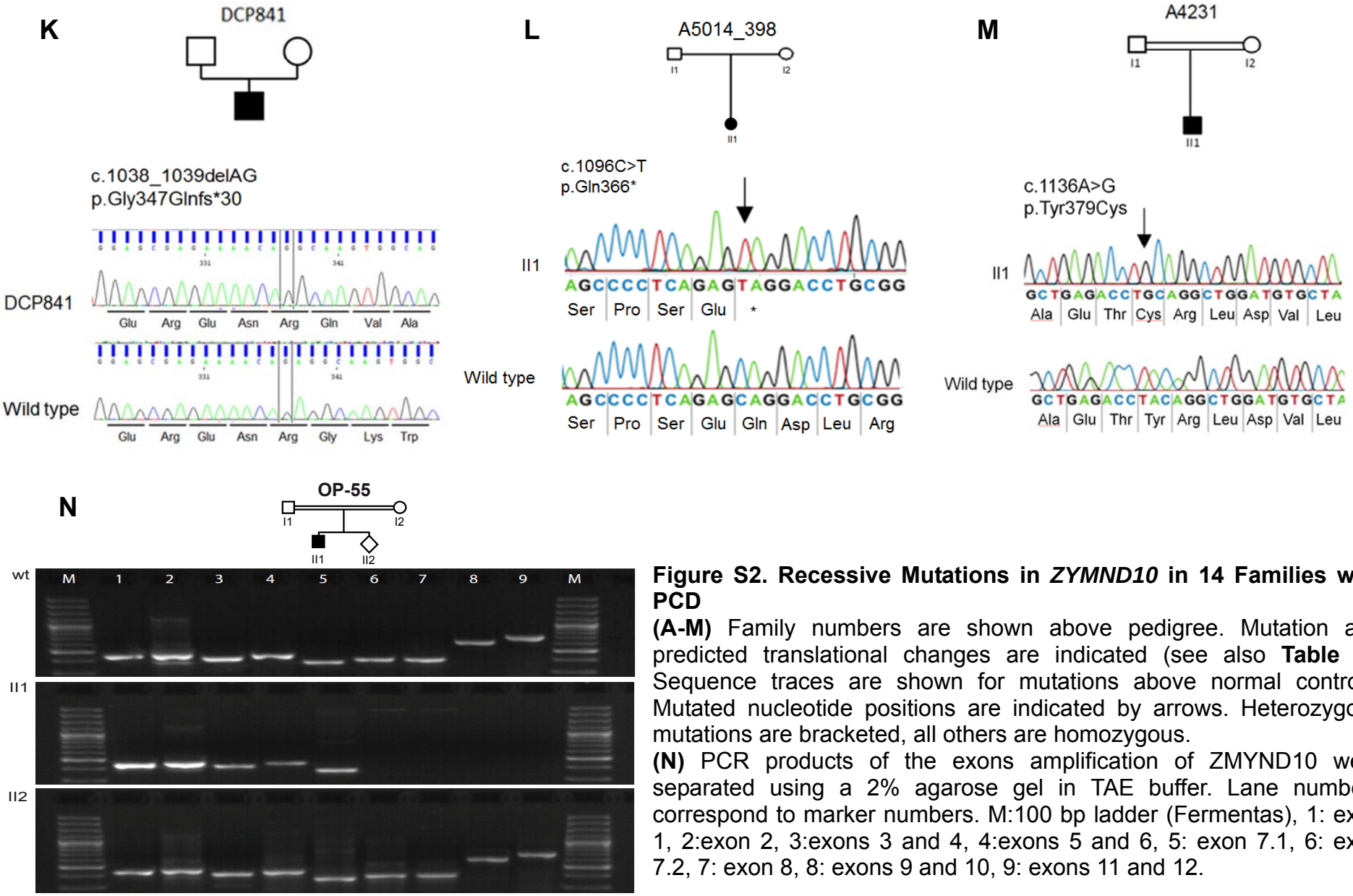

Figure S2. Recessive Mutations in *ZYMND10* in 14 Families with PCD

(A-M) Family numbers are shown above pedigree. Mutation and predicted translational changes are indicated (see also **Table 1**). Sequence traces are shown for mutations above normal controls. Mutated nucleotide positions are indicated by arrows. Heterozygous mutations are bracketed, all others are homozygous.

(N) PCR products of the exons amplification of ZMYND10 were separated using a 2% agarose gel in TAE buffer. Lane numbers correspond to marker numbers. M:100 bp ladder (Fermentas), 1: exon 1, 2:exon 2, 3:exons 3 and 4, 4:exons 5 and 6, 5: exon 7.1, 6: exon 7.2, 7: exon 8, 8: exons 9 and 10, 9: exons 11 and 12.

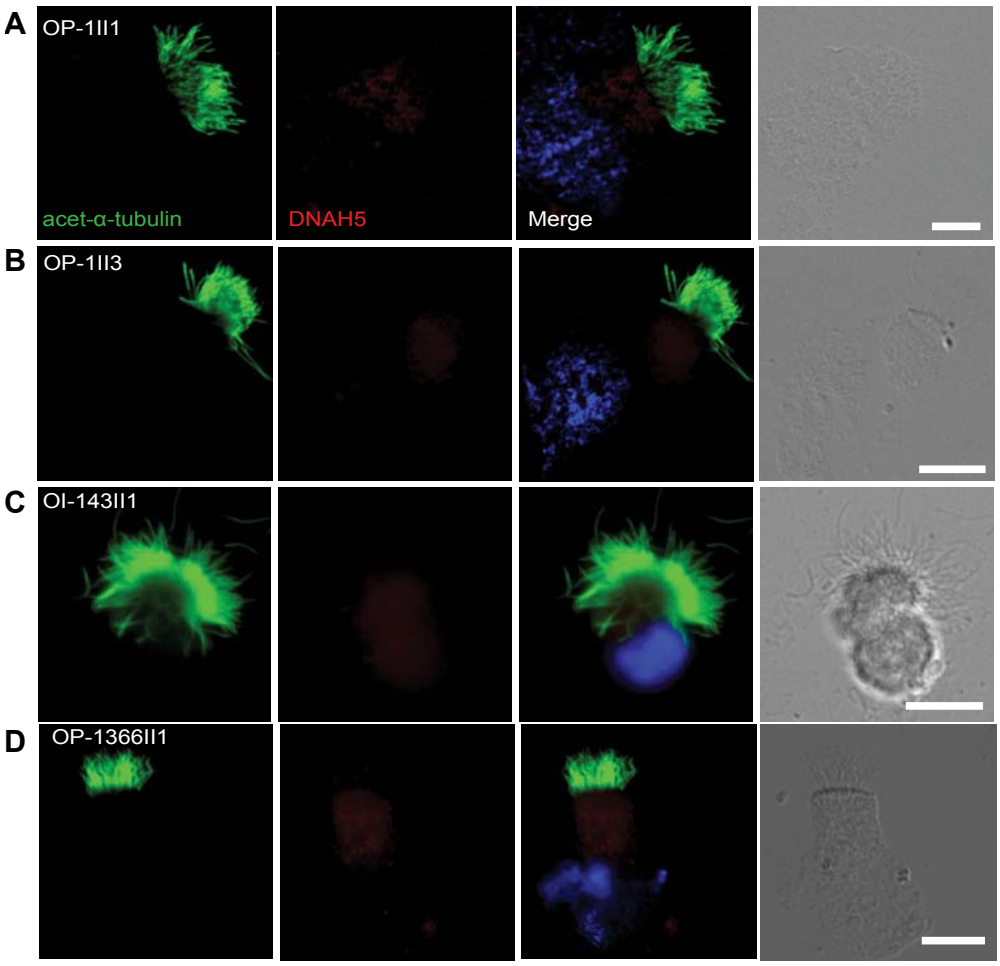

Figure S3. *ZMYND10* Mutations Result in Outer Dynein Arm (ODA) Defects of Respiratory Cilia
Images of respiratory epithelial cells from patients OP-1II1 (A), and OP1-II3 (B), OI143-II1 (C) and OP1366-II1 (D) who carry *ZMYND10* loss-of-function mutations. Cells were co-stained with antibodies against acetylated α-tubulin (green) and DNAH5 (red). Nuclei were stained with Hoechst 33342 (blue). In respiratory cells of patients (**b-g**), DNAH5 is not detectable in the ciliary axonemes, suggesting that *ZMYND10* loss-of-function mutations lead to outer dynein arms defects. Scale bars are 10 μm.

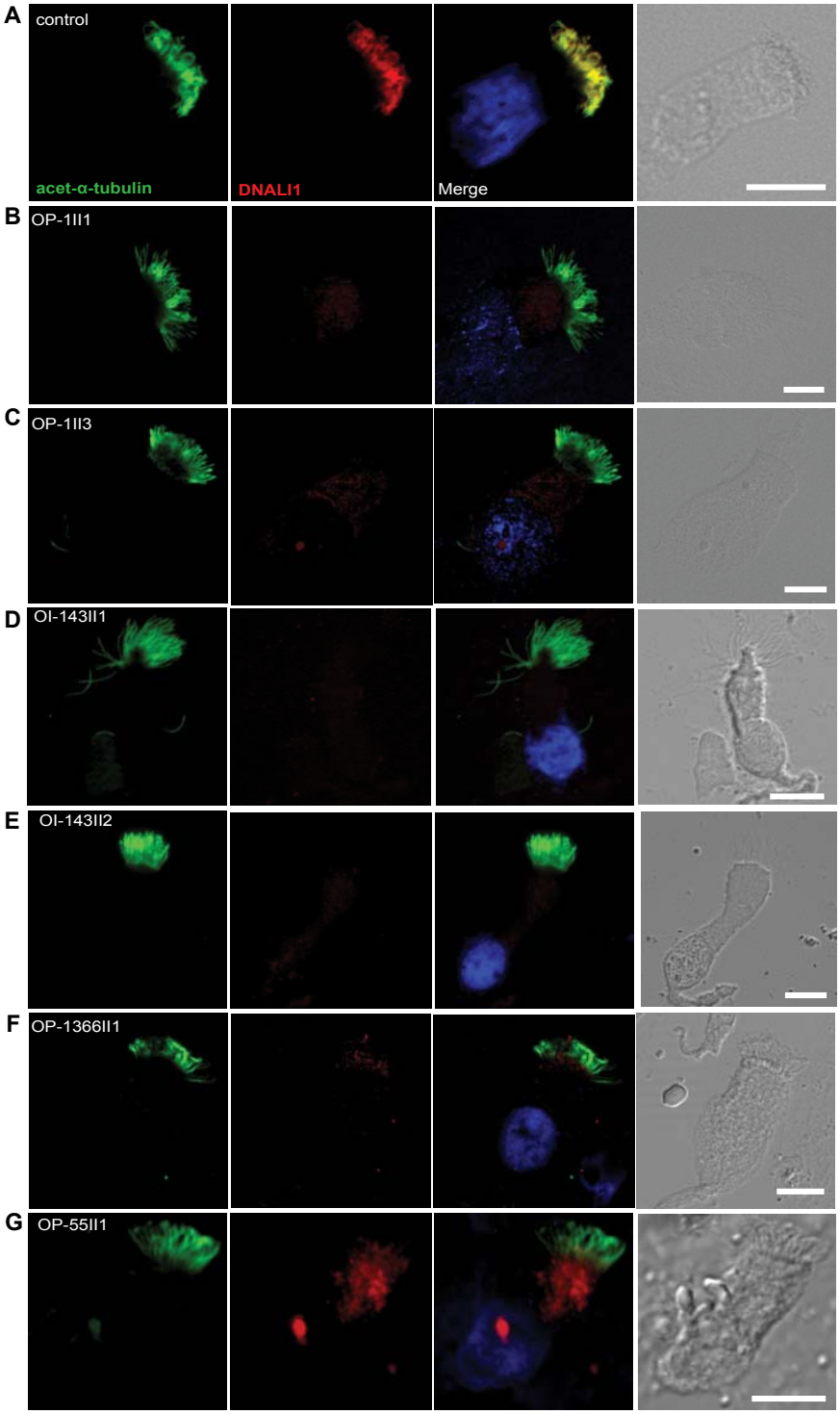

Figure S4. Abnormal Localization of DNALI1 in Respiratory Epithelial Cells from Individuals with PCD Carrying *ZMYND10* Mutations

Images of respiratory epithelial cells from a healthy control (A) and from individuals OP-1 II1 (B), and OP-1 II3 (C), OI-143 II1 (D), OI-143 II2 (E), OP-1366 II1 (F) and OP-55 II1 (G) who carry *ZMYND10* loss-of-function mutations. Cells were co-stained with antibodies against acetylated α-tubulin (green) and DNALI1 (red). Nuclei were stained with Hoechst 33342 (blue). **(A)** In control cells DNALI1 localizes to the axonemes of respiratory cilia. The yellow co-staining within the ciliary axoneme indicates that both proteins co-localize within respiratory cilia. However, in respiratory cells of patients **(B-G)** DNALI1 is not detectable in the ciliary axonemes, suggesting that *ZMYND10* loss-of-function mutations lead to defects in the inner dynein arm light chain DNALI1. Scale bars in A-G, 10μm.

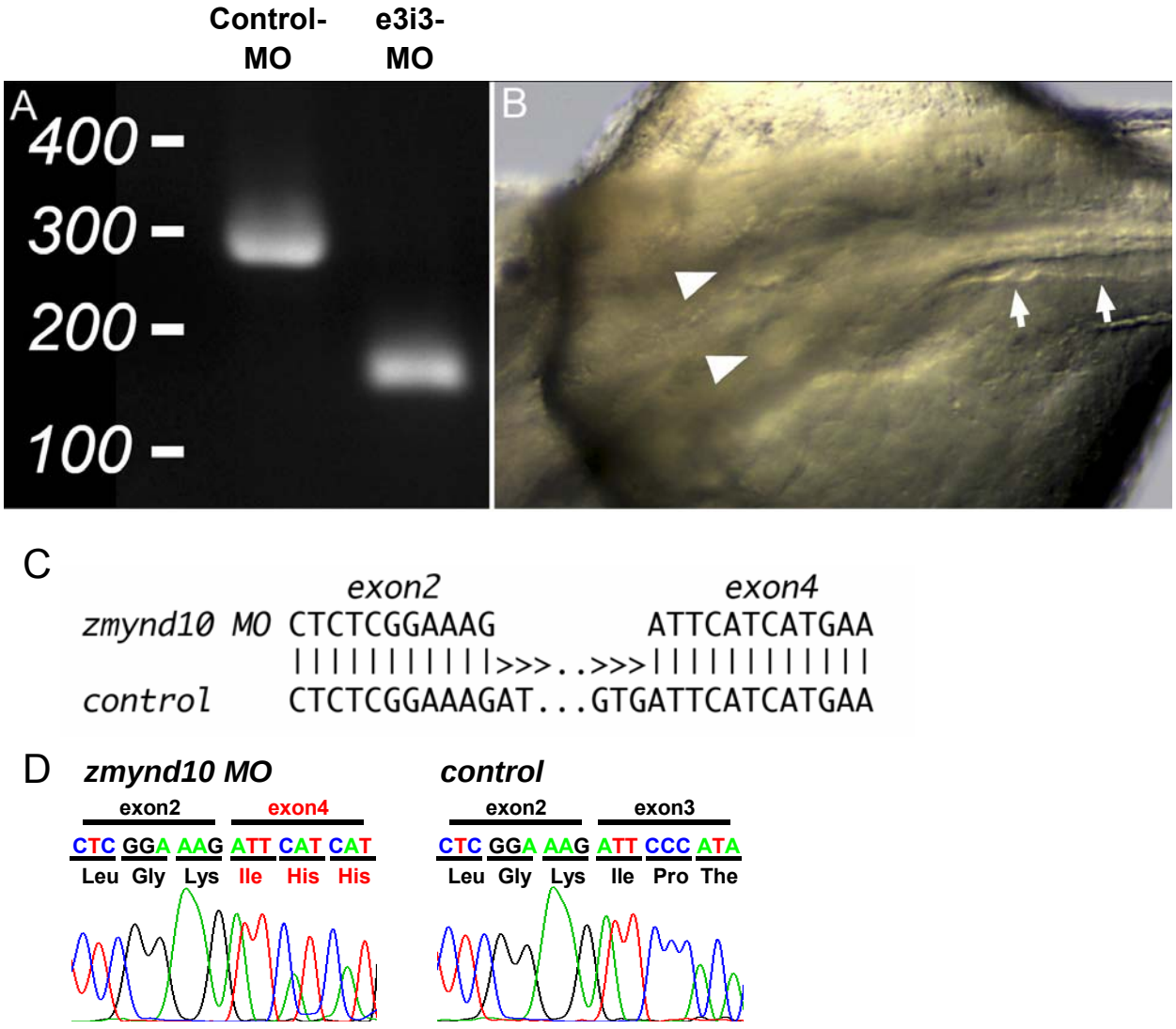

Figure S5. *zmynd10* Knockdown with e3i3 Splice Donor Morpholino
(A) RT-PCR using primers flanking exon 3 revealed a complete absence of wild type *zmynd10* mRNA in e3i3 morpholino injected embryos and a 117 bp deletion product representing an in-frame fusion of exons 2 and 4 (**C** and **D**; exon 3 deletion).
(B) *zmynd10* e3i3 injected embryos show pronephric cysts (arrowheads) and dilated pronephric tubules (arrows), similar to the phenotype observed in *zmynd10* translation blocking morpholino injected embryos.
(C) RT-PCR using primers flanking exon 3 revealed an in-frame fusion of exons 2 and 4 (exon 3 deletion).
(D) Chromatogram of RT-PCR products.

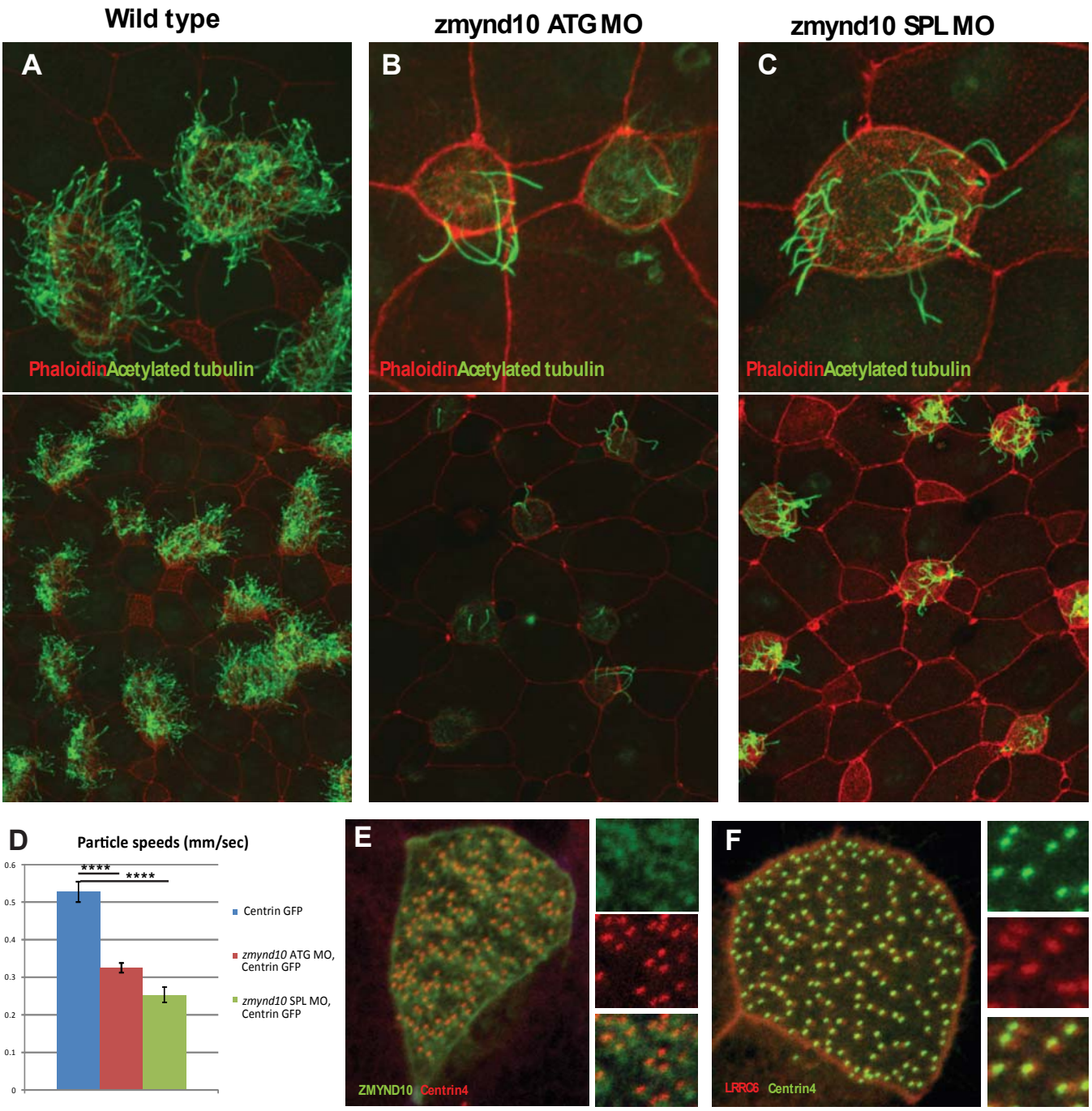

Figure S6. Morpholino Knockdown Phenotype and Localization of *zmynd10*

(A-C) Wild-type and zmynd10 morphant embryos stained with the cilia marker acetylated α-tubulin (green) and the actin marker phalloidin (red). Both the ATG and splice (SPL) morpholinos result in a substantial decrease in cilia number relative to control cells.

(D) Quantification of cilia-generated fluid flow in wild type and morphant embryos. (**** $P < 0.0001$).

(E) Co-localization of GFP-centrin4 (green) with RFP-hsLRRC6 (red) at the basal bodies of *Xenopus* multi-ciliated cells.

(F) Localization of GFP-hsZMYND10 (green) to the basal bodies marked with Centrin4-RFP (red) as well as to the striated rootlets that project away from the basal bodies.

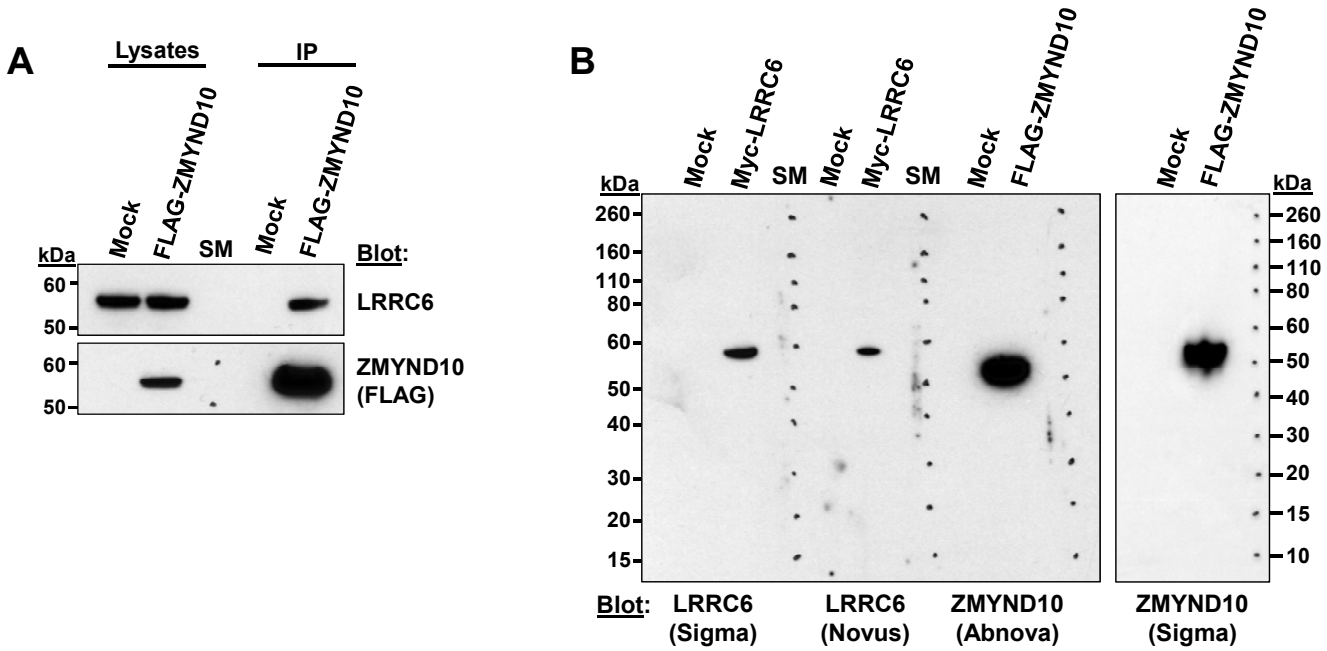

Figure S7. ZMYND10 and LRRC6 Interact with Each Other

(A) Human tracheal epithelial cells (HTEpC) were cultured and transfected with FLAG-ZMYND10 using Cytofect^{TM} (Cell Application, Inc.) according to the manufacturer's protocol. The protein complex precipitated by an anti-FLAG antibody includes endogenous LRRC6 in HTEpC.

(B) Specificity of LRRC6 and ZMYND10 antibodies used in this study. FLAG-tagged *ZMYND10* and Myc-tagged *LRRC6* constructs were transfected into HEK 293T cells. The immunoblots show that antibodies recognize overexpressed proteins and do not give nonspecific bands.

SM denotes size marker.

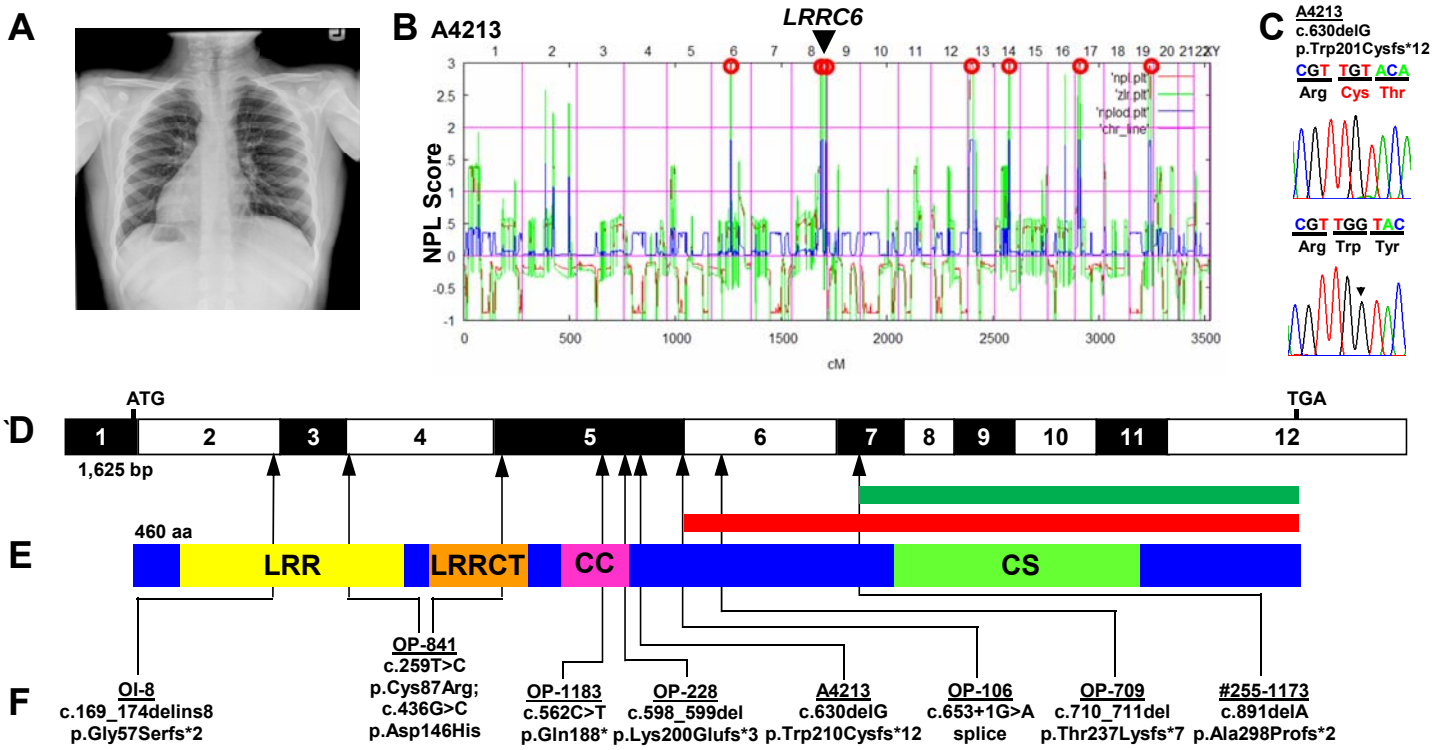

Figure S8. Homozygosity Mapping and Whole Exome Resequencing in PCD Family A4213, and Identification of 7 Different Homozygous and 2 Compound Heterozygous Mutations in *LRRC6* in 13 Families with PCD

(A) Chest X-ray of PCD individual A4213-21 demonstrates *situs inversus*.

(B) For PCD individual A4213 non-parametric lod scores (NPL) from whole genome mapping are plotted across the human genome. The *x*-axis shows Affymetrix 250K *Sty*I array SNP positions on human chromosomes concatenated from *p*-ter (left) to *q*-ter (right). Genetic distance is given in cM. Seven maximum NPL peaks (red circles) indicate candidate regions of homozygosity by descent. Note that the *LRRC6* locus (arrow head) is positioned within one of the maximum NPL peaks on chromosome 8q.

(C) Homozygous *LRRC6* mutation detected in PCD individual A4213-21. Individual number (underlined), mutation (arrowhead), and predicted translational changes are indicated (see also **Table S2**). Sequence trace is shown for mutation above normal controls.

(D) Exon structure of human *LRRC6* cDNA. Positions of start codon (ATG) and of stop codon (TGA) are indicated.

(E) Domain structure of LRRC6 indicates the 4 recognizable domains: LRR (Leucine-rich repeat), LRRCT (C-terminal to leucin-rich repeat), CC (coiled-coil), and CS (CHORD-containing proteins and SGT1). The green and red bars delineate the region necessary for interaction with ZMYND10 (see **Figure 3A**), and DVL3 (see **Figure S13**), respectively.

(F) Nine different homozygous or heterozygous (family OP-841) *LRRC6* mutations detected in 13 families with PCD. Family number (underlined), mutation, and predicted translational changes are indicated (see **Table S2** and **Figure S9**).

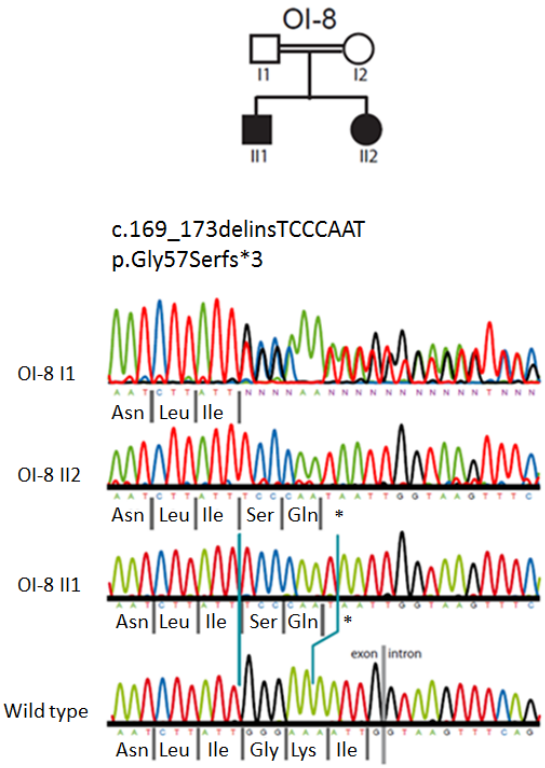
OI-8
I1
I2
II1
II2
c.169_173delinsTCCCAAT
p.Gly57Serfs*3
OI-8 I1
Asn Leu Ile
OI-8 II2
Asn Leu Ile Ser Gln *
OI-8 II1
Asn Leu Ile Ser Gln *
exon intron
Wild type
Asn Leu Ile Gly Lys Ile

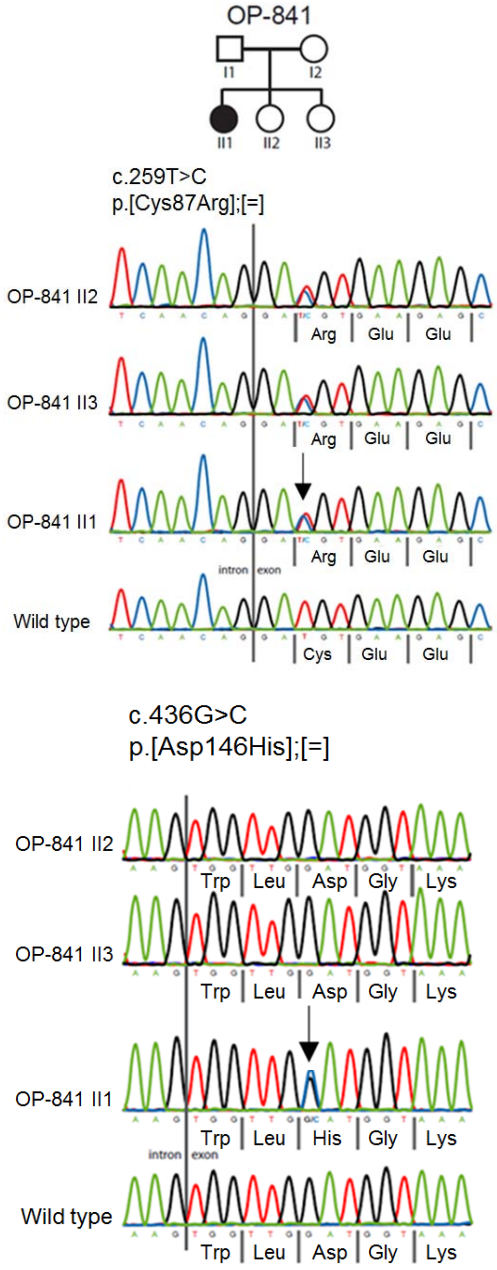
OP-841
I1
I2
II1
II2
II3
c.259T>C
p.[Cys87Arg];[=]
OP-841 II2
Arg Glu Glu
OP-841 II3
Arg Glu Glu
OP-841 II1
Arg Glu Glu
intron exon
Wild type
Cys Glu Glu
c.436G>C
p.[Asp146His];[=]
OP-841 II2
Trp Leu Asp Gly Lys
OP-841 II3
Trp Leu Asp Gly Lys
OP-841 II1
Trp Leu His Gly Lys
intron exon
Wild type
Trp Leu Asp Gly Lys

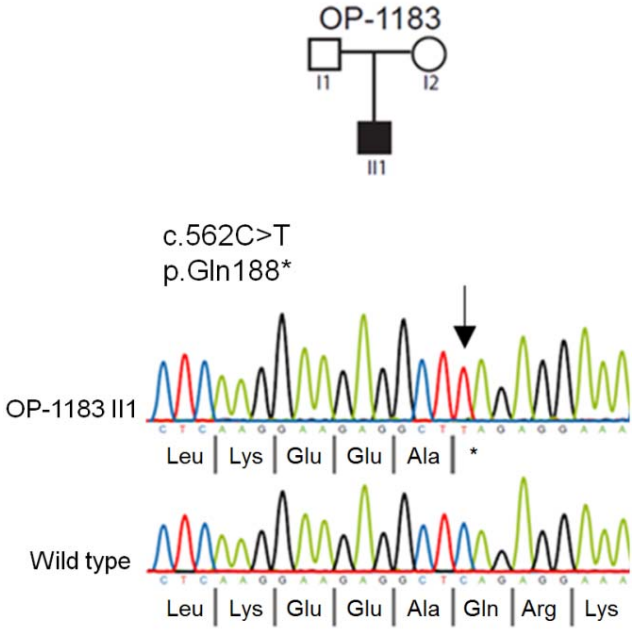
OP-1183
I1
I2
II1
c.562C>T
p.Gln188*
OP-1183 II1
Leu Lys Glu Glu Ala *
Wild type
Leu Lys Glu Glu Ala Gln Arg Lys

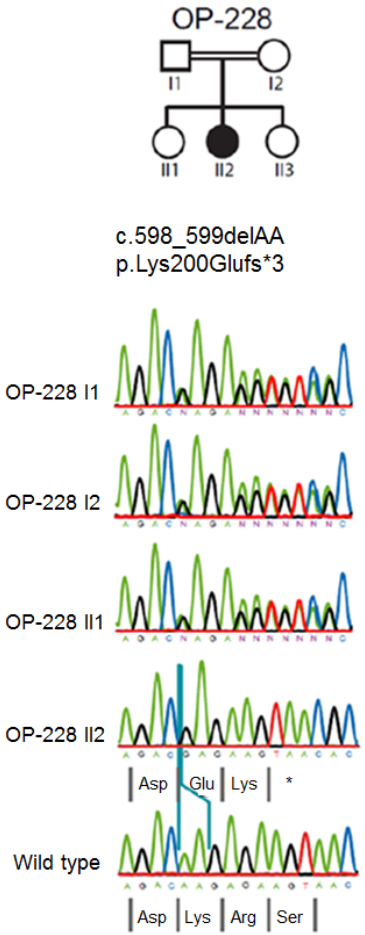
OP-228
I1
I2
II1
II2
II3
c.598_599delAA
p.Lys200Glufs*3
OP-228 I1
OP-228 I2
OP-228 II1
OP-228 II2
Asp
Glu
Lys
*
Wild type
Asp
Lys
Arg
Ser

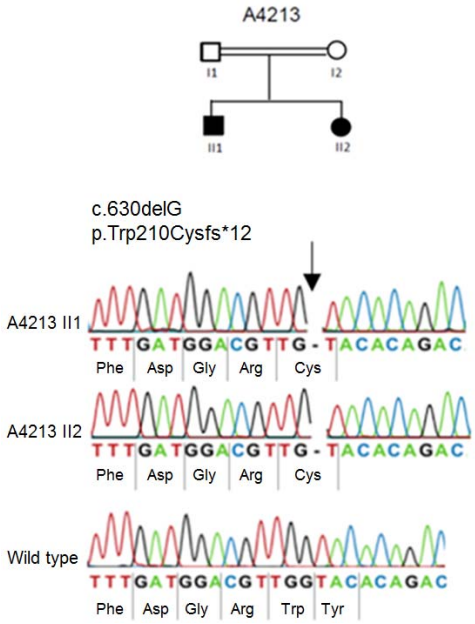
A4213
I1
I2
II1
II2
c.630delG
p.Trp210Cysfs*12
A4213 II1
TTTGATGGACGTTG-TACACAGAC
Phe Asp Gly Arg Cys
A4213 II2
TTTGATGGACGTTG-TACACAGAC
Phe Asp Gly Arg Cys
Wild type
TTTGATGGACGTTGGTACACAGAC
Phe Asp Gly Arg Trp Tyr

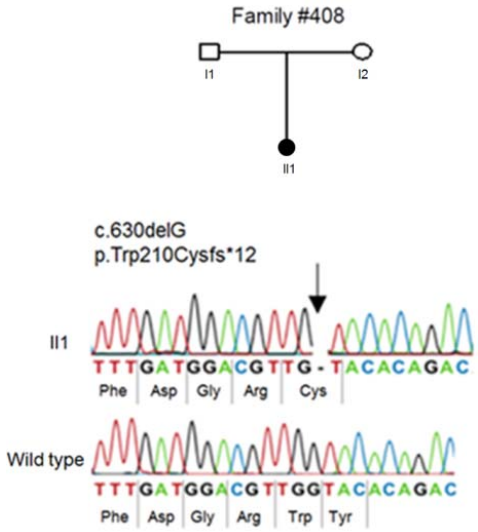
Family #408
I1
I2
II1
c.630delG
p.Trp210Cysfs*12
II1
TTTGATGGACGTTG-TACACAGAC
Phe Asp Gly Arg Cys
Wild type
TTTGATGGACGTTGGTACACAGAC
Phe Asp Gly Arg Trp Tyr

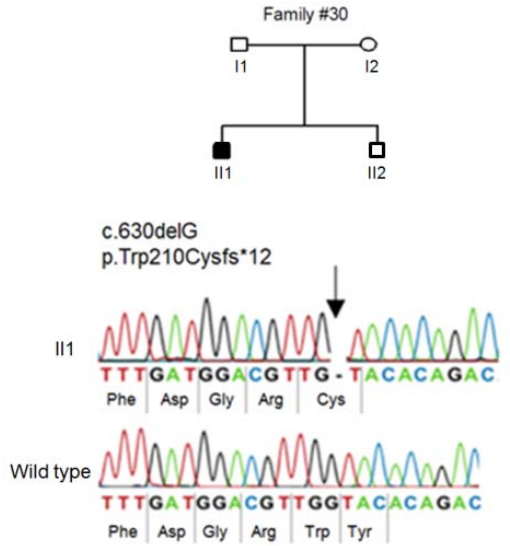
Family #30
I1
I2
II1
II2
c.630delG
p.Trp210Cysfs*12
II1
TTTGATGGACGTTG-TACACAGAC
Phe Asp Gly Arg Cys
Wild type
TTTGATGGACGTTGGTACACAGAC
Phe Asp Gly Arg Trp Tyr

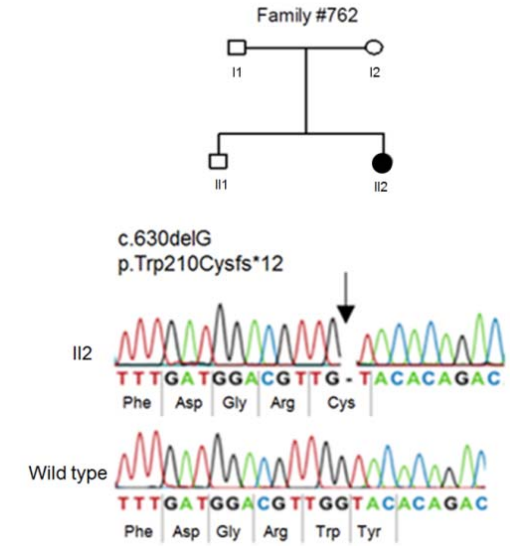
Family #762
I1
I2
II1
II2
c.630delG
p.Trp210Cysfs*12
II2
TTTGATGGACGTTG-TACACAGAC
Phe Asp Gly Arg Cys
Wild type
TTTGATGGACGTTGGTACACAGAC
Phe Asp Gly Arg Trp Tyr

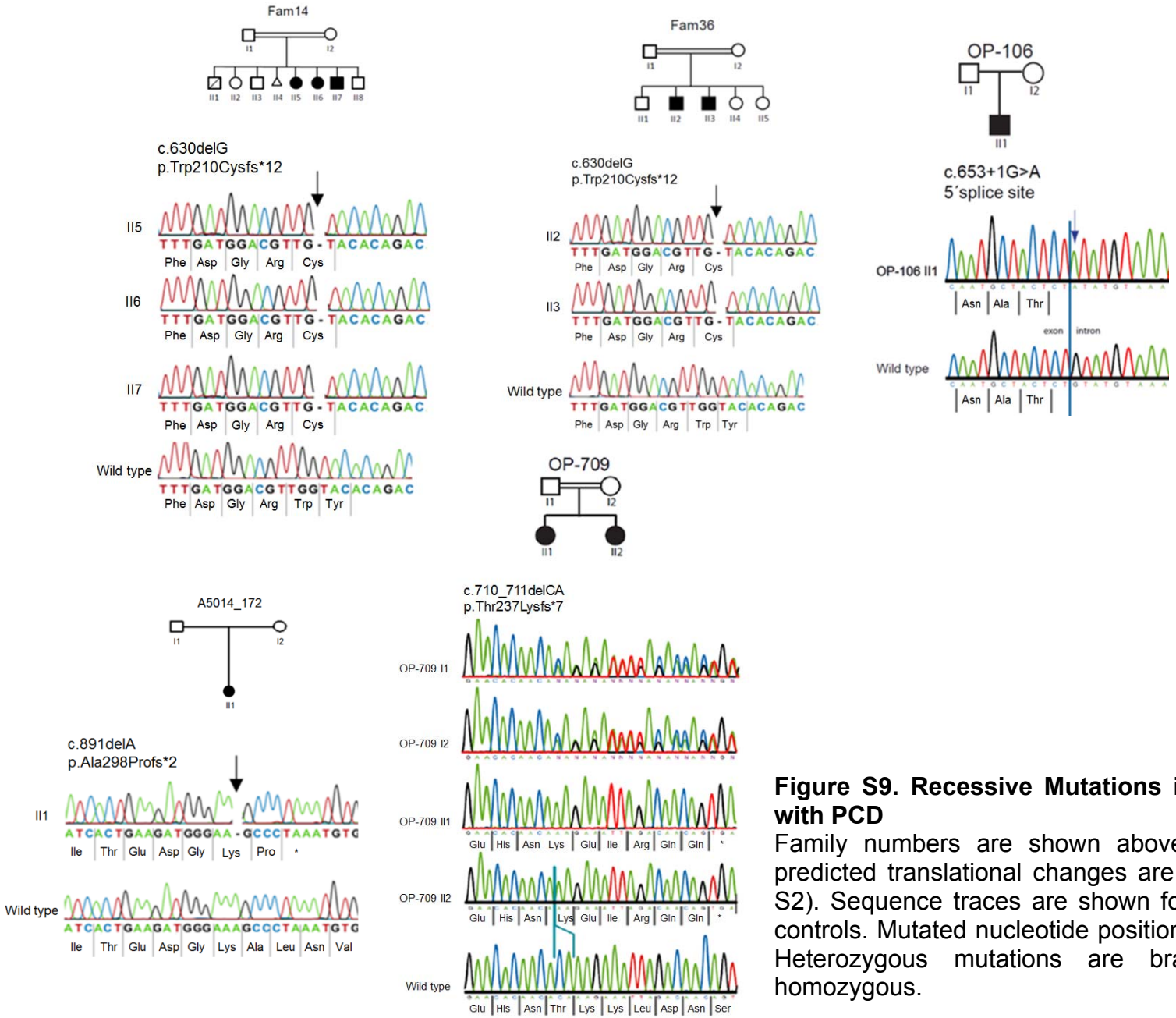

Figure S9. Recessive Mutations in *LRRC6* in 13 Families with PCD

Family numbers are shown above pedigree. Mutation and predicted translational changes are indicated (see also Table S2). Sequence traces are shown for mutations above normal controls. Mutated nucleotide positions are indicated by arrows. Heterozygous mutations are bracketed, all others are homozygous.

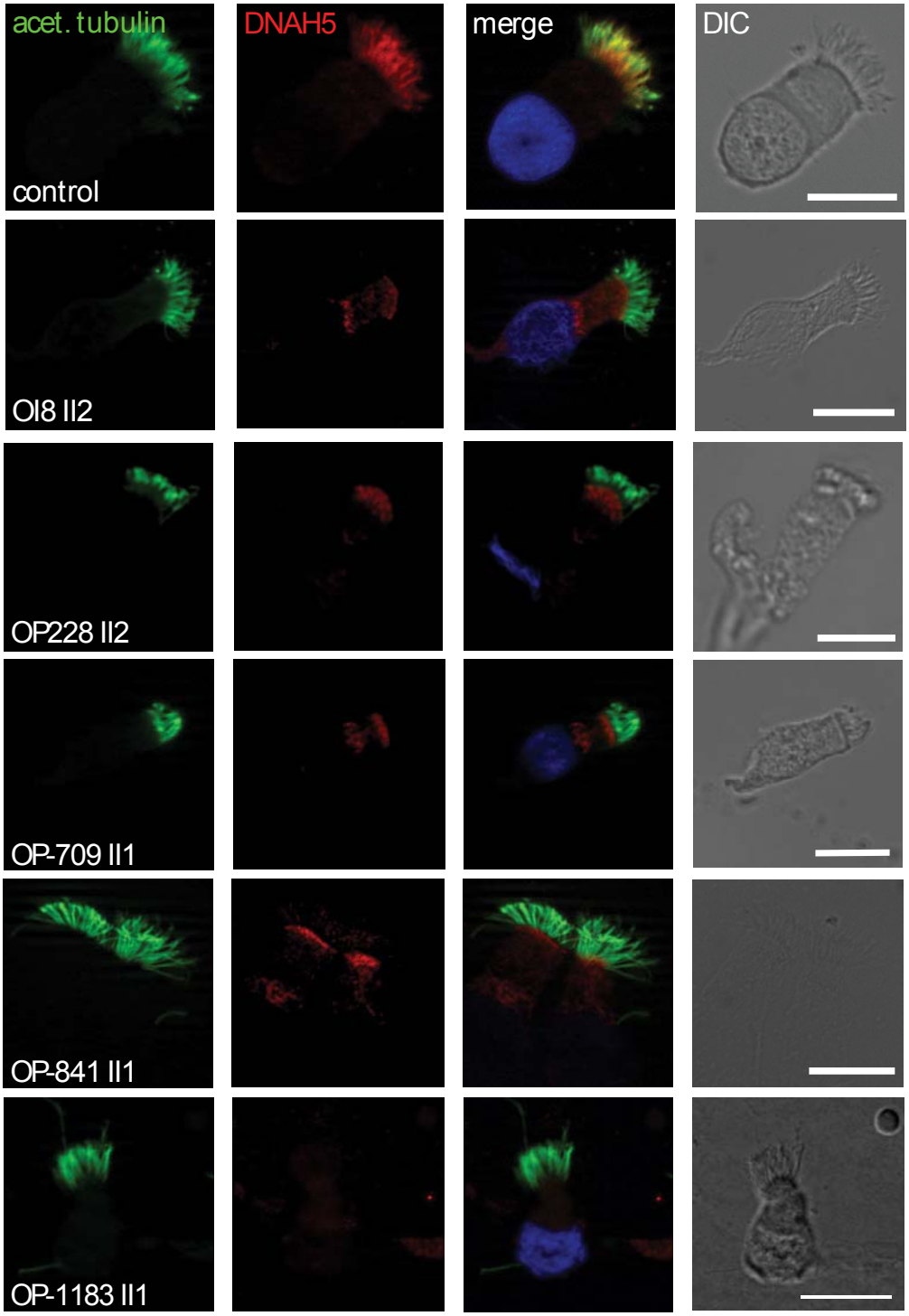

Figure S10. Lack of the Axonemal Outer Dynein arm (ODA) Component DNAH5 in Respiratory Epithelial Cells of Nasal Brushings from PCD Individuals with PCD and *LRRC6* Mutations

High-resolution immunofluorescence microscopy of respiratory cells from a healthy control and individuals with PCD: OI-8 II2, OP-228 II2, OP-709 II1, OP-841 II1, and OP-1183 II1. An antibody directed against outer dynein arm (ODA) heavy chain DNAH5 (present in type 1 and type 2 ODAs) was used (red). As a control for ciliary axonemes, acetylated α-tubulin was stained (green). Note that in *LRRC6* mutant cells, DNAH5 is absent from the axonemes consistent with defects of ODA assembly. Nuclei were stained with Hoechst 33342 (blue). White scale bars represent 10 µm.

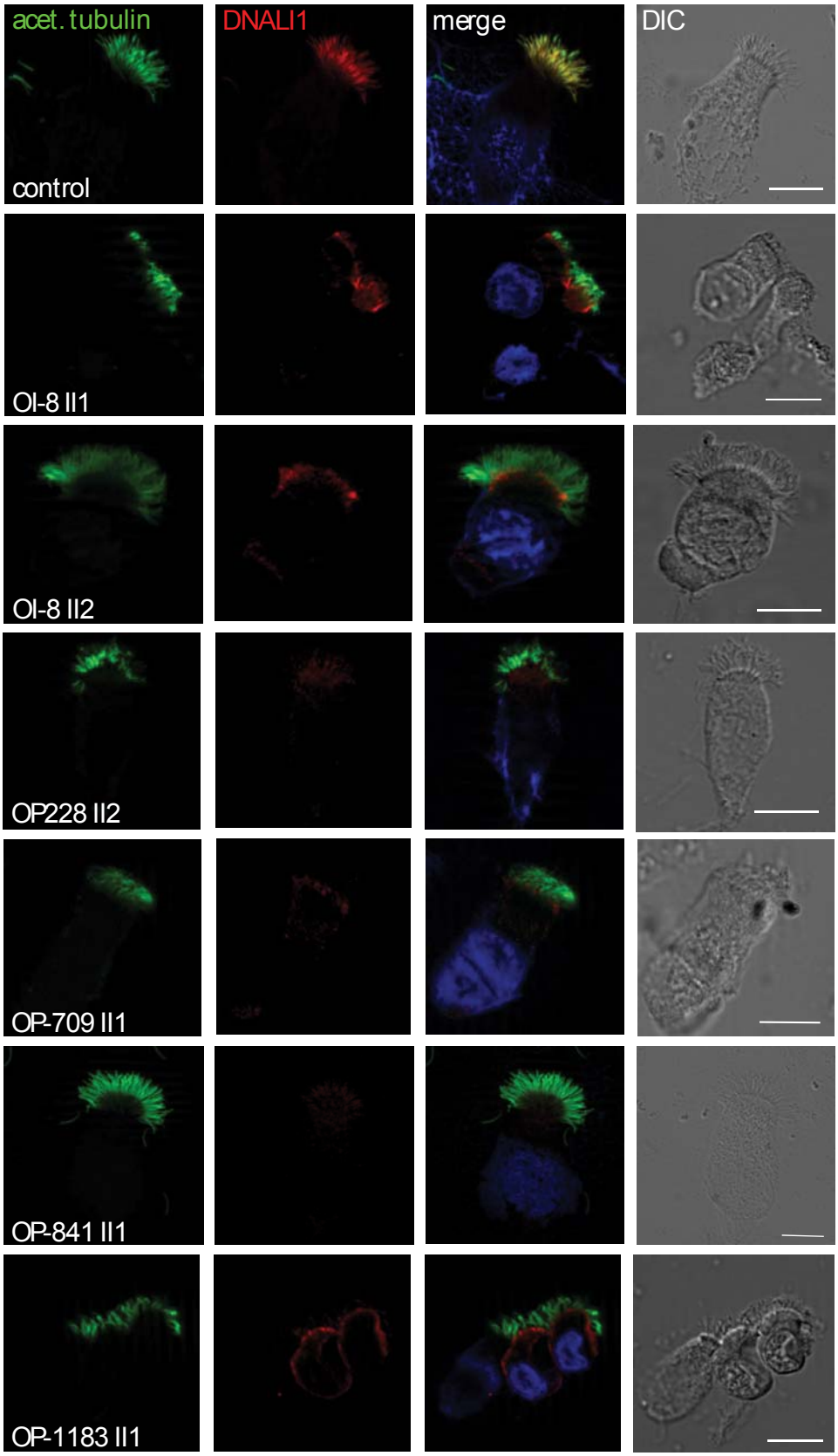

Figure S11. Lack of the Axonemal Inner Dynein Arm (IDA) Component DNALI1 in Respiratory Epithelial Cells of Nasal Brushings from PCD Individuals with PCD and *LRRC6* Mutations

High-resolution immunofluorescence microscopy of respiratory cells from a healthy control and individuals with PCD: OI-8 II1,OI-8 II2, OP-228 II2, OP-709 II1, OP-841 II1, and OP-1183 II1. An antibody directed against IDA light chain DNALI1 was used (red). As a control for ciliary axonemes, acetylated α-tubulin was stained (green). Note that DNALI1 is absent from the axonemes of mutant respiratory cells consistent with assembly defects of DNALI1 containing IDA complexes. Nuclei were stained with Hoechst 33342 (blue). White scale bars represent 10 µm.

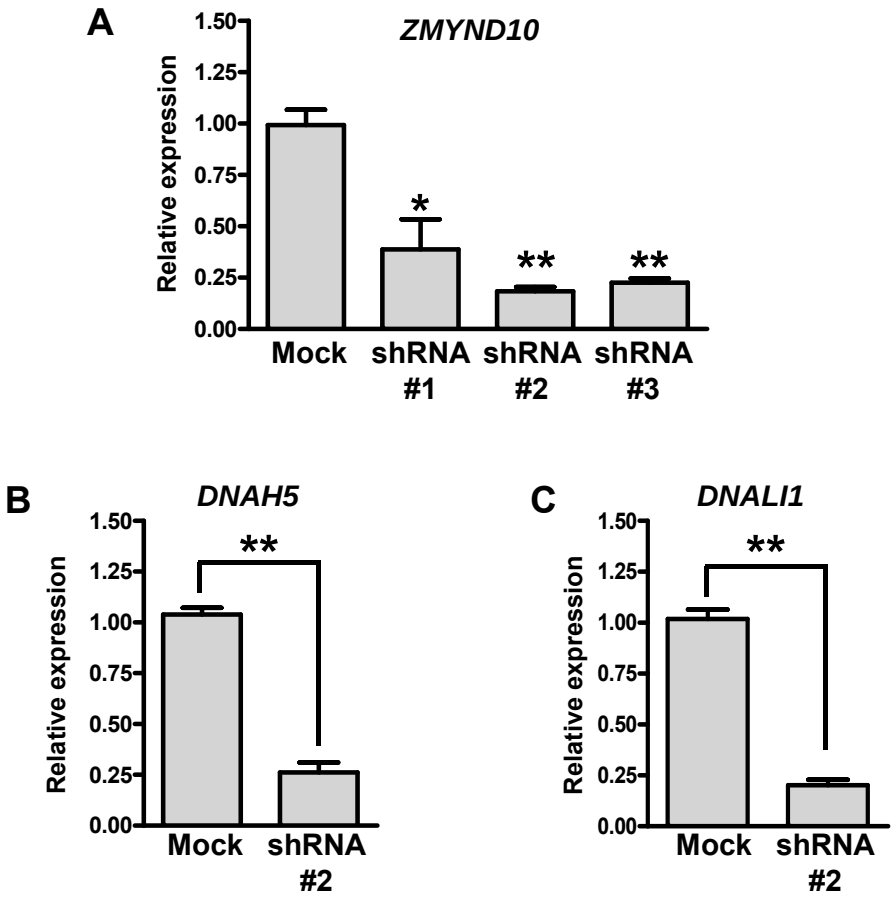

Figure S12. Real-Time PCR Analysis of DNAH5 and DNALI1 Expression in Human Tracheal Epithelial Cells

(A) *ZMYND10*-specific shRNAs were transfected to human tracheal epithelial cells using lentiviral systems. The transfected cells were selected using puromycin. Realtime PCR were performed as previously described.[14] TaqMan probes for *ZMYND10* (Hs01106059_m1), *DNAH5* (Hs00292485_m1), *DNALI1* (Hs00185750_m1), and *glyceraldehyde-3-phosphate dehydrogenase* (*GAPDH*) (Hs02758991_g1) were purchased from Applied Biosystems. The target sequences of shRNAs are GCTACATCACAGACTGTGTGG (shRNA#1), GTCTTGGACTTGGTAGACTAT (shRNA#2) and GGTGTGTGAGTCAGCAGAAGA (shRNA#3).

(B-C) The expression of both ODA component DNAH5 and IDA component DNALI1 was significantly decreased in cells transfected with *ZMYND10*-specific shRNA.

* and ** indicate $p<0.05$ and $p<0.001$ in student t-test compared to control cells.

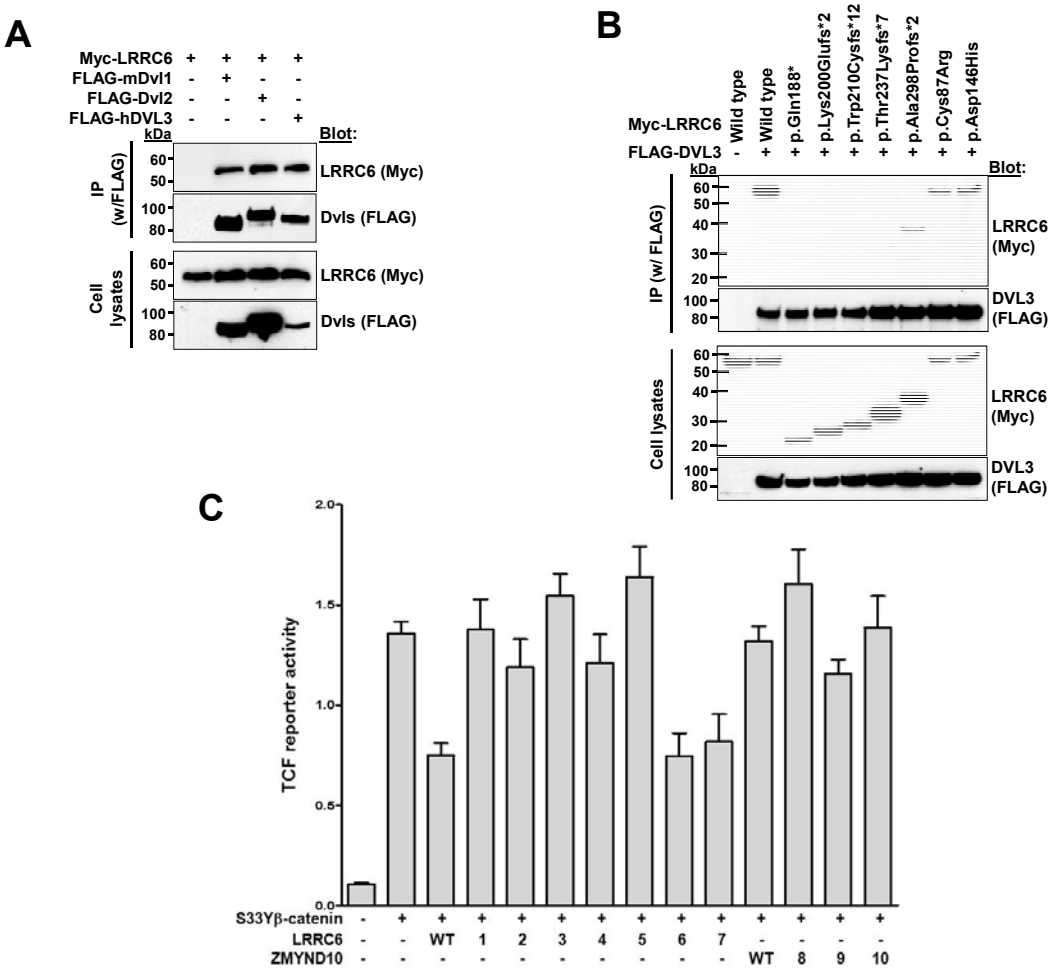

Figure S13. LRRC6 Inhibits β-Catenin-Induced Activation of T Cell Factor (TCF)-Dependent Transcription, but ZMYND10 Does Not

(A) Protein-protein interaction between LRRC6 and Dvls. All of the Dvls (Dvl1, Dvl2 and DVL3) interact with LRRC6.

(B) Protein-protein interaction between LRRC6 and DVL3. Note that the four truncating proteins (p.Gln188*, p.Lys200Glufs*3, p.Trp210Cysfs*12 and p.Thr237Lysfs*7) abrogate interaction with LRRC6, whereas the other three defective proteins (p.Ala298Profs*2, pCys87Arg and p.Asp146His) do not.

(C) Overexpression of LRRC6 WT inhibits β-catenin-induced activation of a TCF-dependent reporter gene. HEK 293 cells were transiently transfected with an empty vector pcDNA3 or pcDNA3-S33Y β-catenin together with LRRC6 (WT and mutants) or ZMYND10 (WT and mutants). Cells were harvested 24 hr later. The ratio between the luciferase activity obtained from the cotransfected TCF-responsive reporter (pTOPFLASH) and the control luciferase reporter gene construct (pGL4.74[hRluc/YK]) was calculated and is designated as "TCF reporter activity". Note that whereas all the truncating proteins (1-5) of LRRC6 fail to inhibit TCF reporter activity, two defective proteins resulting from a missense mutation (6-7) do not show any difference compared to WT. ZMYND10 WT or truncating proteins (8-10) do not have any effect on TCF reporter activity.

The 1-7 in **(C)** are mutants of LRRC6: 1, p.Gln188*; 2, p.Lys200Glufs*3; 3, p.Trp210Cysfs*12; 4, p.Thr237Lysfs*7; 5, p.Ala298Profs*2; 6, p.Cys87Arg; 7, p.Asp146His. The 8-10 in **(C)** are mutants of ZMYND10: 8, p.Phe101Serfs*38; 9, p.Gln323*; 10, p.Gln366*.

Table S1. Biallelic Mutations in Known Genes Associated with PCD in 15 of 31 Families with Homozygosity Mapping Data

Family -Individual[a]	Ethnic origin	Causative Gene	Nucleotide alteration	Deduced protein change	Exon (Zygosity)	Parental consan-guinity	Clinical and ultrastructural findings
Mutations in known genes associated with PCD							
A4197 (#8) -21 (#50) -23 (#49)	Caucasian	***DNAH5***	**c.1090-6A>G** **c.6230T>C**	**p.(?)** (splice acceptor site, predicted by Human Splicing Finder) **p.Phe2077Ser**	Intron 8 (het) 37 (het)	No	ODA defect
A4233 (#647) **-** 21 (#1978) - 22 (#1979)	Caucasian/Mormon	***DNAH5***	**c.5983C>T** **c.8498G>A**	**p.Arg1995*** **p.Arg2833His**	36 (het) 51 (het)	No	ODA defects in >60% of cilia
A4201 (#20) **-**21 (#153) **-**22 (#154)	Caucasian	***DNAH5***	c.6249G>A **c.10384C>T**	p.Met2083Ile (80% conserved splice donor) **p.Gln3462***	37 (het) 61 (het)	No	ODA defect -21: +SI
A4207 (#100) **-**21 (#618) -22 (#619)	Caucasian	***DNAH5***	**c.9427A>T** c.10615C>T	**p.Lys3143*** p.Arg3539Cys	56 (het) 63 (het)	No	ODA defect
A4200 (#11) -22 (#72) -23 (#71)	German-Mennonites	***DNAH5***	**c.10384C>T**	**p.Gln3462***	61 (Hom)	Yes	ODA defects -22: SI
A4293 (#1) -21 (#1) -22 (#2) -23 (#3)	Caucasian	***CCDC39***	c.610-2A>G (Intron 5) **c.830_831delCA**	p.(?) (100% conserved splice acceptor site) **p.Thr277Argfs*3**	Intron 5 (het) 7 (het)	No	IDA defects with microtubular disorganization -21: +SI
A4195 (#2) -21 (#10) -22 (#11)	Caucasian	***CCDC39***	**c.1528-1543A>G** **c.1540_1544delTTTAT**	**p.(?)** (novel spice acceptor site, predicted by Human Splicing Finder) **p.Phe514Glnfs*5**	12 (het) 12 (het)	No	IDA defects with microtubular disorganization -21: +SI
A4199 (#10) -21 (#66) -22 (#67)	Caucasian	***CCDC39***	**c.1789G>T** (13) **c.2497_2498delCA**	**p.Glu597*** (h) **p.Gln833Valfs*6**	13 (het) 18	No	IDA defects with microtubular disorganization -21: +SI

			(18)	(h)	(het)		
A4220 (#337) **-**21 (#1310) -22 (#1311)	Caucasian	***CCDC40***	c.248delC	p.Ala83Valfs*84	3 (Hom)	No	IDA defects with microtubular disorganization -22: +SI
A4216 (#250) **-**21 (#1166) -22 (#1167)	South Asian	***CCDC40***	**c.1416delG**	**p.Ile473Phefs*2**	9 (Hom)	Yes	IDA defects with microtubular disorganization
A4208 (#130) **-**21 (#818) -23 (#820)	Caucasian	***CCDC40***	c.2441G>A	p.Arg814*	14 (Hom)	Yes	IDA defects with microtubular disorganization -21: +SI
A4224 (#394) **-**21 (#1439) -22 (#1670)	Caucasian/ Hispanic	***DNAH11***	**c.2491C>T** **c.3871G>A**	**p.Gln831*** **p.Ala1291Thr**	14 (het) 21 (het)	No	Normal DA+CA -22 : SI
A4230 (#560) -22 (#1737) **-**23 (#1736)	Caucasian	***DNAH11***	**c.4438C>T** **c.8698C>T**	p.Arg1480* **p.Arg2907***	25 (het) 54 (het)	No	Normal DA+CA -23: +SI
A4218 (#268) **-**21 (#1192) -23 (#1193)	Caucasian	***DNAI2***	**c.1304G>A** **c.1357_1358insG**	p.Trp435* **p.Glu453Glyfs*40**	10 (het) 11 (het)	No	ODA defect
A4217 (#264) **-**21 (#1186)	South Asian	***CCDC103***	c.461A>C	p.His154Pro	4 (Hom)	Yes	possible ODA defects
Heterozygous only mutations in known genes associated with PCD							
A4228 (#530-1674) **-**21 (#9115) -22 (#9116)	Caucasian	***DNAH5***	**c.4237C>T**	**p.Gln1413***	27 (het)	No	ODA defect -22: SA
A4198 (#9) -21 (#62) -22 (#63)	Caucasian	***DNAH5***	c.5647C>T	p.Arg1883*	34 (het)	No	ODA defect -21: +SI -22: +SA
A4221 (#348) -21 (#1332) -22 (#1442)	Caucasian	***DNAH5***	**c.8449-2A>G**	**p.(?)** (100% conserved splice acceptor site)	Intron 50 (het)	No	ODA defect -21:SI

ODA, outer dynein arm; IDA, inner dynein arm; SI, *situs inversus*; SA, *situs ambiguous*; DA, dynein arm; CA, central apparatus

[a]Individual with exome capture data is underlined in first column.

GenBank accession numbers. The following GenBank accession numbers were used for annotation of recessive mutations: *DNAH5*: NM_001369.2, *CCDC39*: NM_181426.1, *CCDC40*: NM_017950.3, *DNAH11*:NM_003777.3, *DNAI2*: NM_023036.4, *CCDC103*: NM_213607.2.

Mutations which are not reported in HGMD® Gene Mutation Database are shown in bold.

Table S2. Biallelic Mutations of *LRRC6* in 13 Families with Primary Ciliary Dyskinesia

Family -Individual	Ethnic origin	Nucleotide alteration [a,b] (segregation)	Deduced protein Change	Exon/ Intron (Zygosity)	AA sequence conservation[c]	Parental consanguinity	IF (axonemal ODA/IDA protein localization)	TEM	Video-Microscopy	Other (clinical features)
OI-8 -II1 -II2	Israeli	c.169_173delinsTCCCAAT (-11: het, -12: ND)	p.Gly57Serfs*3	2 (Hom)	N/A	Yes	**DNAH5**: defect **DNALI1**: defect	ODA+IDA defects	immotile cilia	-21/-22: SI, recur. sinusitis/pneumonia, BE
OP-841	Danish	c.259T>C c.436G>C	p.Cys87Arg p.Asp146His	4 (het) 5 (het)	Drosophila Drosophila	No	**DNAH5**: defect **DNALI1**: defect	ODA+IDA defects	immotile cilia	SS, BE
OP-1183	Turkish	c.562C>T	p.Gln188*	5 (Hom)	N/A	ND	**DNAH5**: defect **DNALI1:** defect	ODA+IDA defects	immotile cilia	SI, BE, recur. bronchitis/rhinitis, infertility
OP-228 -II2	German	c.598_599delAA (-11: het, -12: het)	p.Lys200Glufs*3	5 (Hom)	N/A	Yes	**DNAH5**: defect **DNALI1**: defect	-	immotile cilia	SI, recur. otitis media /pneumonia, PRDS
A4213 (#232) -21 (#1143) -22 (#1144)	Asian-Pakistani	**c.630delG** (-11: ND, -12: het)	p.Trp210Cysfs*12	5 (Hom)	N/A	Yes	ND	ODA+IDA defects	ND	-21: SI
#30 -21 (#204)	Asian-Pakistani	c.630delG (-11: het, -12: het)	p.Trp210Cysfs*12	5 (Hom)	N/A	No	ND	ODA+IDA defects	immotile cilia	SS
#408 -21 (#1465)	Asian-Pakistani	c.630delG	p.Trp210Cysfs*12	5 (Hom)	N/A	No	ND	ODA+IDA defects	ND	SI
#762 -21 (#2190)	Asian-Pakistani	c.630delG	p.Trp210Cysfs*12	5 (Hom)	N/A	No	ND	ODA+IDA defects	ND	SI +multiple pancreas
Fam9 -25, -26, -27	Asian-Pakistani	c.630delG (-11: het, -12: het)	p.Trp210Cysfs*12	5 (Hom)	N/A	Yes	ND	ODA+IDA defects	-	SS
Fam21 -22, -23	Asian-Pakistani	c.630delG (-11: het, -12: het)	p.Trp210Cysfs*12	5 (Hom)	N/A	Yes	ND	ODA+IDA defects	-	SS
OP-106	Turkish	c.653+1G>A	oblig. 5´splice site	5 (Hom)	N/A	Yes	ND	ND	ND	SA, PRDS
OP-709 -II2 -II1	Turkish	c.710_711delCA (-11: het, -12: het)	p.Thr237Lysfs*7	6 (Hom)	N/A	Yes	**DNAH5**: defect **DNALI1:** defect	ND	ND	-22/-21:SA/SS, complex CHD, recur. pneumonia/sinusitis /otitis media, PRDS
A5014_172 (#255) -21 (#1173)	Caucasian	c.891delA	p.Ala298Profs*2	7 (Hom)	N/A	No	ND	ODA+IDA defetcs	ND	SS

[a]The mutation in the index family is **bold**. Recurrent mutations are underlined. [b]cDNA mutations are numbered according to human cDNA reference sequence NM_012472.3 (*LRRC6*), where +1 corresponds to the A of ATG start translation codon. [c]Amino acid (AA) residue is continually conserved throughout evolution as indicated.

BE, Bronchiectasis, CHD, congenital heart defect; het, heterozygous; Hom, homozygous; IDA, inner dynein arm; IF, immunofluorescence; N/A, not applicable; ND, no data; ODA, outer dynein arm; PRDS, postnatal respiratory distress syndrome, SA, *situs ambiguous*; SI, *situs inversus*; SS, *situs solitus*; TEM, transmission electron microscopy.

Table S3. Primer/Morpholino Sequences for Zebrafish MO Knockdown

Target	**Primer sequence** (5'→3')	**Product size (bp)**
zmynd10	zmynd10 RTPCR F1	GGTGGTTTCGCCAGCATGAATTT
zmynd10	zmynd10 RTPCR R1	TCCAGATACAGAGCGTCCCACCA
zmynd10	zmynd10 RTPCR F2	GCGCCAATCAGGAGGAATTCATTA
zmynd10	zmynd10 RTPCR R2	CCAGCAGTGTGAGTTTGCGATGA
zmynd10	zmynd10 ATG MO	ACTGAATCCATCGCTTCAGAATGTT
zmynd10	zmynd10 e3i3 splice junction MO	TAAGCTGAGTCTGCTCACCACCATG

F, forward; R, reverse.

Table S4. Detailed Demographic and Clinical Phenotype in PCD Patients Tested for *LRRC6*

Clinical observation		PCD patients with ODA+IDA defect tested for *LRRC6*	
		Full gene by Sanger sequencing*	**Restriction digestion for 630delG mutation§**
Subjects	Total # of patients	4 (100%)	36 (100%)
Gender	Male	2 (50%)	18 (50%)
	Female	2 (50%)	18 (50%)
Age Range		27 - 48 years	3 months - 68 years
Parental consanguinity		1 (25%)	4 (11%)
Ethnicity	Caucasian	2 (50%)	25 (69%)
	Non-Caucasian	2 (50%)†	11 (31%)‡
Situs status	Situs inversus	1 (25%)	18 (50%)
	Situs ambiguus	0	4 (11%)
	Situs solitus	3 (75%)	14 (39%)
Neonatal RDS‖	Yes	3 (100%)	30 (83%)
	No	0	6 (17%)
Bronchiectasis‖	Yes	4 (100%)	19 (66%)
	No	0	10 (34%)
Sinusitis‖	Yes	4 (100%)	22 (63%)
	No	0	13 (37%)
Otitis Media‖	Yes	2 (50%)	28 (78%)
	No	2 (50%)	8 (22%)
Nasal NO (nl/min)‖	Mean±SD	22.0±17.53††	16.88±13.25††
	(# of subjects)	4 (100%)	28 (78%)

* All coding exons and splice junction were interrogated.

§ c.630delG (p.W210CfsX11) creates a BsrG1 restriction site that was used to interrogate patients.

† Included 1 Asian and 1 Brazilian ethnicity.

‡ Included 7 Asian, 1 African American, 2 Hispanic, and 1 mixed Caucasian/American Indian Alaskan ethnicity.

‖ Incomplete information on some of the patients.

†† Normal nasal NO levels, calculated from 27 healthy subjects 376+124nl/min (mean+SD) {Ref:listed as MZ6}.

Abbreviations:

ODA+IDA = Outer+inner dynein arms, NO = Nitric Oxide, SD = Standard Deviation